



Evolution of genome structure in the *Drosophila simulans* species complex

Mahul Chakraborty, Ching-Ho Chang, Danielle E. Khost, et al.

Genome Res. 2021 31: 380-396 originally published online February 9, 2021

Access the most recent version at doi:[10.1101/gr.263442.120](https://doi.org/10.1101/gr.263442.120)

References This article cites 210 articles, 66 of which can be accessed free at:
<http://genome.cshlp.org/content/31/3/380.full.html#ref-list-1>

Open Access Freely available online through the *Genome Research* Open Access option.

Creative Commons License This article, published in *Genome Research*, is available under a Creative Commons License (Attribution 4.0 International), as described at <http://creativecommons.org/licenses/by/4.0/>.

Email Alerting Service Receive free email alerts when new articles cite this article - sign up in the box at the top right corner of the article or [click here](#).

To subscribe to *Genome Research* go to:
<https://genome.cshlp.org/subscriptions>

Evolution of genome structure in the *Drosophila simulans* species complex

Mahul Chakraborty,^{1,7} Ching-Ho Chang,^{2,7,8} Danielle E. Khost,^{2,3}
 Jeffrey Vedanayagam,⁴ Jeffrey R. Adrion,⁵ Yi Liao,¹ Kristi L. Montooth,⁶
 Colin D. Meiklejohn,⁶ Amanda M. Larracuente,² and J.J. Emerson¹

¹Department of Ecology and Evolutionary Biology, University of California Irvine, Irvine, California 92697, USA; ²Department of Biology, University of Rochester, Rochester, New York 14627, USA; ³FAS Informatics and Scientific Applications, Harvard University, Cambridge, Massachusetts 02138, USA; ⁴Department of Developmental Biology, Memorial Sloan-Kettering Cancer Center, New York, New York 10065, USA; ⁵Institute of Ecology and Evolution, University of Oregon, Eugene, Oregon 97403, USA; ⁶School of Biological Sciences, University of Nebraska-Lincoln, Lincoln, Nebraska 68502, USA

The rapid evolution of repetitive DNA sequences, including satellite DNA, tandem duplications, and transposable elements, underlies phenotypic evolution and contributes to hybrid incompatibilities between species. However, repetitive genomic regions are fragmented and misassembled in most contemporary genome assemblies. We generated highly contiguous de novo reference genomes for the *Drosophila simulans* species complex (*D. simulans*, *D. mauritiana*, and *D. sechellia*), which speciated ~250,000 yr ago. Our assemblies are comparable in contiguity and accuracy to the current *D. melanogaster* genome, allowing us to directly compare repetitive sequences between these four species. We find that at least 15% of the *D. simulans* complex species genomes fail to align uniquely to *D. melanogaster* owing to structural divergence—twice the number of single-nucleotide substitutions. We also find rapid turnover of satellite DNA and extensive structural divergence in heterochromatic regions, whereas the euchromatic gene content is mostly conserved. Despite the overall preservation of gene synteny, euchromatin in each species has been shaped by clade- and species-specific inversions, transposable elements, expansions and contractions of satellite and tRNA tandem arrays, and gene duplications. We also find rapid divergence among Y-linked genes, including copy number variation and recent gene duplications from autosomes. Our assemblies provide a valuable resource for studying genome evolution and its consequences for phenotypic evolution in these genetic model species.

[Supplemental material is available for this article.]

Repetitive DNA sequences comprise a substantial fraction of the genomes of multicellular eukaryotes, occupying >40% of human and *Drosophila melanogaster* genomes (Britten and Kohne 1968; International Human Genome Sequencing Consortium 2001; Treangen and Salzberg 2012; Hoskins et al. 2015). These sequences include repeated tandem arrays of noncoding sequences like satellite DNAs, self-replicating selfish elements like transposable elements (TEs), and duplications of otherwise unique sequences, including genes (Britten and Kohne 1968). Despite being historically considered nonfunctional, repetitive sequences are now known to play significant roles in both cellular and evolutionary processes. In many eukaryotes, satellite DNA, tandem repeats, and/or TEs constitute structures essential for genome organization and function, like centromeres and telomeres (Moyzis et al. 1988; Mason et al. 2008; Klein and O'Neill 2018; Chang et al. 2019; Hartley and O'Neill 2019). Short tandem repeats near protein-coding genes can regulate gene expression by recruiting transcription factors (Rockman and Wray 2002; Gemayel et al. 2010), and euchromatic satellite repeats contribute to X Chromosome recogni-

tion during dosage compensation in *Drosophila* males (Menon and Meller 2012; Menon et al. 2014).

In both humans and fruit flies, genetic polymorphism composed of repetitive sequences makes up a larger proportion of the genome than all single-nucleotide variants (SNVs) combined (The 1000 Genomes Project Consortium 2015; Chakraborty et al. 2018). Moreover, repetitive sequence variants can have significant fitness effects, underlie ecological adaptations, drive genome evolution, and participate in genomic conflicts (e.g., Daborn et al. 2002; Aminetzach et al. 2005; Montchamp-Moreau et al. 2006; Tao et al. 2007a,b; Fishman and Saunders 2008; Larracuente and Presgraves 2012; Ellison and Bachtrog 2013; Van't Hof et al. 2016; Battlay et al. 2018; Chakraborty et al. 2018, 2019). The selfish proliferation of repetitive sequences can alter protein-coding genes (Lipatov et al. 2005), create intragenomic conflicts (Doolittle and Sapienza 1980; Orgel and Crick 1980), and trigger evolutionary arms races within and between genomes (Werren et al. 1988; Aravin et al. 2007; Ellis et al. 2011; Cocquet et al. 2012; Lindholm et al. 2016; Blumenstiel 2019; Parhad and Theurkauf 2019; Rathje et al. 2019). For example, centromeric repeats can drive through female meiosis, causing rapid evolution of centromere proteins to restore equal segregation (Henikoff et al. 2001). Repeats can also be the target of selfish meiotic drivers in males (e.g., Larracuente and Presgraves 2012), which may drive

⁷These authors contributed equally to this work.

⁸Present address: Division of Basic Sciences, Fred Hutchinson Cancer Research Center, Seattle, WA 98109, USA
 Corresponding authors: alarracu@ur.rochester.edu, jje@uci.edu

Article published online before print. Article, supplemental material, and publication date are at <https://www.genome.org/cgi/doi/10.1101/gr.263442.120>. Freely available online through the *Genome Research* Open Access option.

© 2021 Chakraborty et al. This article, published in *Genome Research*, is available under a Creative Commons License (Attribution 4.0 International), as described at <http://creativecommons.org/licenses/by/4.0/>.

the rapid evolution of these repeats to escape the driver (e.g., Cabot et al. 1993; Larracuente 2014). The lack of recombination and male-limited transmission of Y Chromosomes also create opportunities for conflicts involving repetitive DNA to evolve, such as sex-chromosome meiotic drive. Such conflicts have driven the proliferation of sex-linked gene families in mammals and *Drosophila* (Cocquet et al. 2012; Kruger et al. 2019; for review, see Jaenike 2001). These conflicts may also impose selection pressures that trigger the rapid turnover of Y-linked repeats (Lohe and Roberts 1990; Bachtrog 2004; Larracuente and Clark 2013; Mahajan et al. 2018; Wei et al. 2018).

The very nature of repetitive sequences makes them difficult to study. Whole-genome shotgun sequencing of reads shorter than common repeats yields erroneous, fragmented, and incomplete genome assemblies in repetitive regions (Hoskins et al. 2002, 2015; Salzberg and Yorke 2005; Alkan et al. 2011; Treangen and Salzberg 2012). Reference-quality genomes have historically been available only for distantly related species, making it difficult to investigate the evolutionary dynamics of repetitive sequences (for review, see Plohl et al. 2012; Lower et al. 2018). Long-read-based assemblies help solve these challenges because they can be nearly complete, contiguous, and accurate even in repetitive genomic regions (Steinberg et al. 2014; Berlin et al. 2015; Chaisson et al. 2015; Chakraborty et al. 2016, 2018; Mahajan et al. 2018; Solares et al. 2018; Chang and Larracuente 2019).

To understand the contributions of repetitive sequences to genome structure and evolution, we sequenced and assembled reference-quality genomes of *Drosophila simulans*, *Drosophila sechellia*, and *Drosophila mauritiana*. These three species, collectively

known as the *Drosophila simulans* species complex (or sim-complex) (Kliman et al. 2000), comprise the nearest sister species to *D. melanogaster* and are virtually equally related to each other (Fig. 1A), likely as a consequence of rapid speciation (Garrigan et al. 2012; Pease and Hahn 2013). The four fruit fly species together comprise the *D. melanogaster* species complex (or mel-complex) (Hey and Kliman 1993). The mel-complex serves as a model system for studying speciation (Tao et al. 2001; Wu 2001; Meiklejohn et al. 2018), behavior (Ding et al. 2019), population genetics (Kliman et al. 2000; Begun et al. 2007; Garrigan et al. 2012), and molecular evolution (Moriyama and Powell 1997; Ranz et al. 2007; Hu et al. 2013). All four species are reproductively isolated from one another, producing either sterile or lethal hybrids (Barbash 2010). They show unique ecological adaptations: *D. sechellia* larvae specialize on a host fruit toxic to most other *Drosophila* species (R'Kha et al. 1991), whereas *D. melanogaster* larvae can thrive in ethanol concentrations lethal to the sim-complex species (Merçot et al. 1994). In euchromatic regions, these species show ~95% sequence identity (Begun et al. 2007; Garrigan et al. 2012). However, the degree of interspecific divergence in repetitive genomic regions that are not represented in current assemblies is unknown (Chakraborty et al. 2018; Miller et al. 2018).

Here we use high-coverage long-read sequencing to assemble sim-complex genomes de novo, permitting us to resolve repetitive regions that have, until now, evaded scrutiny. These assemblies are comparable in completeness and contiguity to the latest release of the *D. melanogaster* reference genome. Our results uncover a dynamic picture of repetitive sequence evolution that leads to extensive genome variation over short timescales.

Results

Contiguous, accurate, and complete assemblies resolve previous misassemblies

We collected deep (100- to 150-fold autosomal coverage) long-read sequence data from adult male flies (Supplemental Fig. S1, S2; Supplemental Table S1) to assemble reference-quality genomes de novo for the three sim-complex species. Our assemblies are as contiguous as the *D. melanogaster* reference (Fig. 1B; Supplemental Fig. S3; Supplemental Table S2; Hoskins et al. 2015). In all three species, single contigs span the majority of each chromosome arm, except the X Chromosome in *D. sechellia*. Our scaffolds include the entirety of the euchromatin and large stretches of pericentric heterochromatin (Figs. 1B, 2; Supplemental Fig. S4). We assembled >20 Mbp of pericentric heterochromatin (Fig. 2A), overcoming difficulties associated with these genomic regions (Khost et al. 2017; Chang et al. 2019).

Comparison of our assemblies to the *D. melanogaster* genome recovers synteny expected between the species across major chromosome arms (Fig. 2A,B; Supplemental Fig. S4). Genome-wide, ~15% of sim-complex genome content fails to align uniquely to *D. melanogaster*. Within aligned sequence blocks, the sim-complex species show ~7% divergence from *D. melanogaster* (Supplemental Fig. S5). Preservation of synteny between the genomes suggests that there are no large errors, which is further supported by the evenly distributed long-read coverage (Supplemental Figs. S1, S2) and mapping of BAC sequences across the assembled chromosomes (Supplemental Fig. S6; Supplemental Information, methods and analyses). We corrected errors previously noted in the draft assemblies of these species (Supplemental Fig. S7; Supplemental Table S3), including a ~350-kb 3L subtelomeric fragment

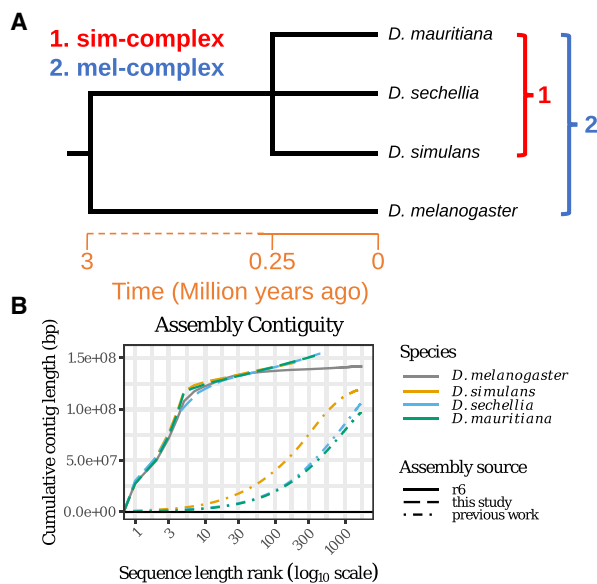


Figure 1. Reference-quality de novo genome assemblies of the *Drosophila melanogaster* species complex. (A) Phylogeny showing the evolutionary relationship among the members of four mel-complex species. (B) Contiguities of the new assemblies from the sim-complex and the reference assembly of *D. melanogaster* (R6). The contigs were ranked by their lengths, and their cumulative lengths were plotted on the y-axis. The colors represent different species. The *D. melanogaster* genome is the release 6 assembly (Hoskins et al. 2015). For previous work, *Drosophila simulans* is ASM75419v3 (Hu et al. 2013), *Drosophila sechellia* (r1.3) is from *Drosophila* 12 Genomes Consortium (2007), and *Drosophila mauritiana* is from Garrigan et al. (2014).

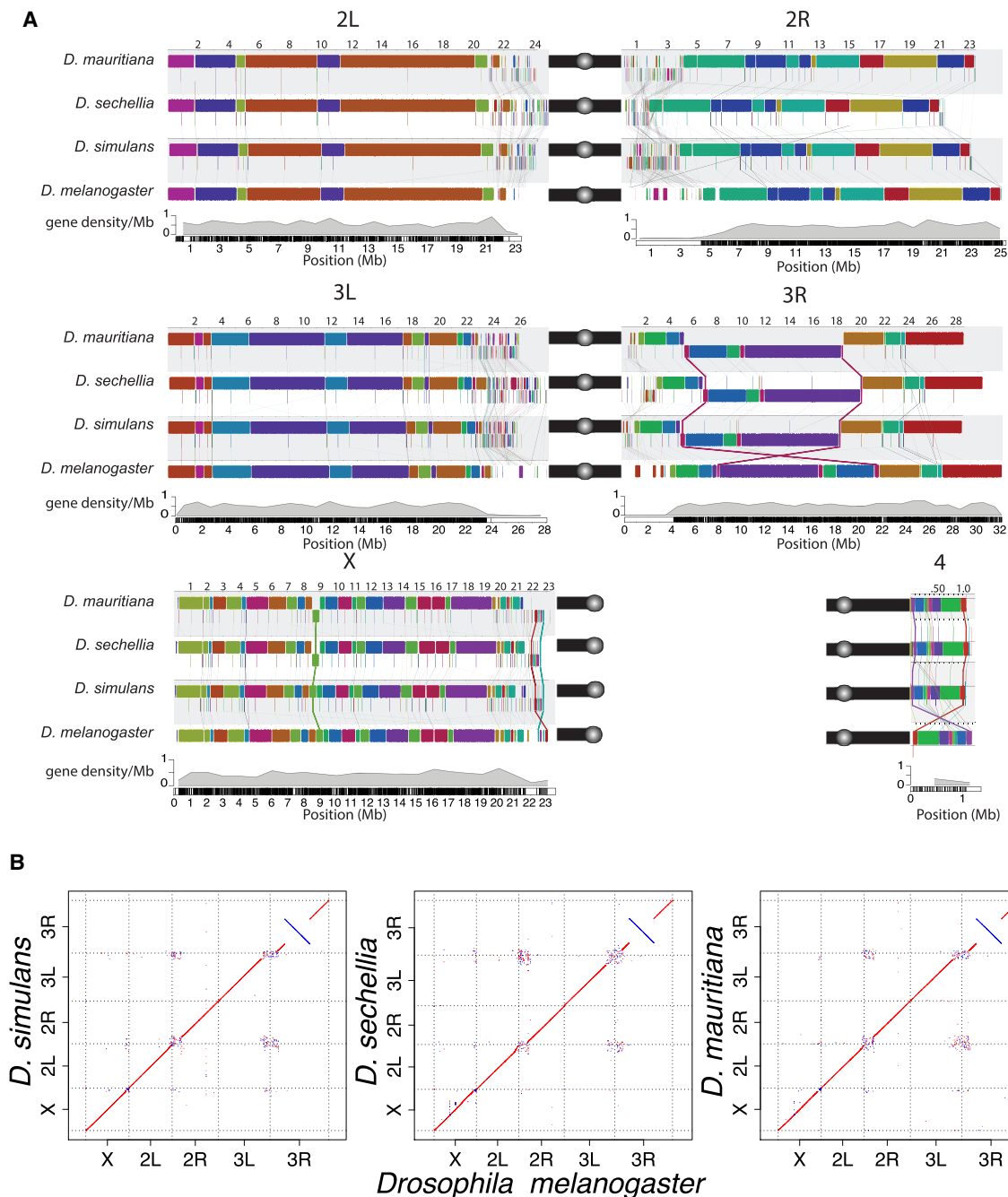


Figure 2. Chromosomal rearrangements in the sim-complex species. We used Mauve (A) and minimap2 (B) (Li 2018) to show synteny between the members of the sim-complex and *D. melanogaster*. (A) Colored rectangles show positions of syntenic collinear blocks free from internal rearrangements compared with the *D. melanogaster* reference (r6; see details in Methods). Each chromosome arm is plotted with its own scale, with the position in megabases indicated above each chromosome. Blocks that appear below the black line are in an inverse orientation. Lines connect homologous colored blocks between genomes, and crossing lines indicate structural rearrangements. Along the euchromatic chromosome arms, there are three major inversion events (X, 3R, and 4). The heterochromatic regions have significantly more rearrangements than the euchromatin (see text). Pericentromeric heterochromatic regions are marked with a solid black bar, and the circles correspond to centromeres. (B) The dot plots for the whole genome and each chromosome arm between the sim-complex species and *D. melanogaster*.

misassembled onto the 2R scaffold in the previous *D. simulans* assembly (Schaeffer et al. 2008). Our assemblies are also highly accurate at the nucleotide level, as concordance between our assemblies and Illumina data is comparable to that of *D. mel-*

nogaster (cf. QV = 44.0–46.3 for sim-complex species vs. 44.3 for *D. melanogaster*) (Supplemental Table S4). The sim-complex assemblies are highly complete, with numbers of single-copy conserved Dipteran orthologs (BUSCO) (Simão et al. 2015) comparable to

that of *D. melanogaster* (98.6%–99% BUSCO) (Supplemental Table S5). Moreover, we detected more *D. melanogaster* orthologous genes in our sim-complex assemblies compared with the previous assemblies (Supplemental Table S6; Supplemental Information, methods and analyses).

We also assembled entire *Wolbachia* genomes from *D. mauritiana* (wMau) and *D. sechellia* (wSech) (Supplemental Table S7); our *D. simulans* w^{XD1} strain was not infected with *Wolbachia*. Our assemblies reveal extensive and previously unknown structural divergence between closely related *Wolbachia* genomes. wSech is 95.1% identical to wHa (supergroup A) from *D. simulans*. We detect a single inversion differentiating wSech from wHa (Supplemental Fig. S8A). wMau is 95.8% identical to wNo from *D. simulans* (supergroup B) and is >99.9% identical to other recently published *Wolbachia* genomes from *D. mauritiana* (available from NCBI GenBank [<https://www.ncbi.nlm.nih.gov/genbank/>] under accession numbers CP034334 and CP034335) (Lefoulon et al. 2019). We infer extensive (15) structural rearrangement events between recently diverged *Wolbachia* lineages, wNo and wMau, under the double-cut-and-join (DCJ) model (Supplemental Fig. S8B; Lin and Moret 2008). A recent study of *Wolbachia* from different isolates of *D. mauritiana* identified four deletions in wMau relative to wNo (Meany et al. 2019). Our assemblies indicate that these deletions are associated with other SVs. Three of the four deletions (CNVs 1, 3, and 4 in Supplemental Fig. S8C) occur at rearrangement breakpoints, whereas the fourth (CNV 2) shows a segment repeated in wNo flanking the segment deleted in wMau. Finally, wMau maintains a single-copy segment in one of the deletions (CNV 1), which itself is a dispersed duplication in wNo (Supplemental Fig. S8C). It remains unclear whether any of these structural changes contribute to the lack of fecundity effects or cytoplasmic incompatibility caused by infection with wMau (Meany et al. 2019).

Clade- and species-specific genomic rearrangements

We computed locally collinear alignment blocks with Mauve (Lin and Moret 2008) to infer genomic rearrangements between species. We discovered 535–542 rearrangements between *D. melanogaster* and the sim-complex (approximately 90 mutations per million years), and 113–177 rearrangements within the sim-complex (226–354 mutations per million years) (Supplemental Table S8). Heterochromatic regions harbor 95% of all genomic rearrangements (Supplemental Fig. S9; Supplemental Table S8). In euchromatin, there is an enrichment of rearrangements on the X Chromosome: 63% of all identified rearrangements (17/27) between *D. melanogaster* and the sim-complex species and all but one (12/13) rearrangement within the sim-complex species are X-linked (Fig. 2A; Supplemental Table S8).

Within euchromatin, *D. simulans*, *D. mauritiana*, and *D. sechellia* differ from *D. melanogaster* by 23, 25, and 21 inversions, respectively. We recovered the 13.6-Mb *D. melanogaster*-specific 3R inversion (In(3R)84F1; 93F6–7; 3R:8,049,180–21,735,108) that was initially characterized cytologically (Sturtevant and Plunkett 1926) and confirmed by breakpoint cloning (Fig. 2; Ranz et al. 2007). Among nine inversions shared in all sim-complex species, four are also present in the outgroup species *Drosophila yakuba* and *Drosophila ananassae*, suggesting that they occurred in the *D. melanogaster* lineage. The remaining five are found only in the sim-complex species. The sim-mau, sim-sec, and mau-sec species pairs share five, three, and four euchromatic inversions absent in the third species, respectively. For example, *D. sechellia* and

D. mauritiana, but not *D. simulans*, share a 460-kb X-linked inversion (X:8,744,323–9,203,725 and X:8,736,133–9,203,526, respectively) spanning 45 protein-coding genes (Fig. 2; Supplemental Fig. S10A).

We also observe evidence for two large (>100-kb) inversions within pericentromeric heterochromatin on Chromosomes 3 and X (Fig. 2; Supplemental Fig. S11A–D). Because *Drosophila erecta* shares the same configuration as the sim-complex species, the pericentric inversion on Chromosome 3 likely occurred in the *D. melanogaster* lineage (Supplemental Fig. S12). We also observed an ~700-kb inversion in the X heterochromatin of sim-complex species spanning 35 genes (22.4–23.1 Mb on *D. melanogaster* X) (Fig. 2A,B; Supplemental Figs. S4B,H,N, S10). This inversion is sim-complex specific and is absent in *D. melanogaster*, *D. yakuba*, and *D. erecta*. We also find large, species-specific heterochromatic inversions on 3R in *D. sechellia* (Fig. 2A,B; Supplemental Fig. S11A, B) and 2R in *D. mauritiana* (Supplemental Fig. S13).

Repetitive DNA

Our annotations of repetitive DNA (Supplemental File S1) revealed substantially greater repeat abundance in the sim-complex genomes compared with older assemblies of these species (Supplemental Fig. S14). On the five large chromosome arms, the density of repetitive elements increases approaching the euchromatin–heterochromatin boundary, consistent with patterns of TE density in *D. melanogaster* (Fig. 3; Kaminker et al. 2002; Bergman et al. 2006). Below we describe our analyses of the different classes of repetitive elements.

Distribution of satellites

We identified three novel complex satellite arrays in the sim-complex, which we named for their monomer size (90U, 193XP, and 500U). 500U is located primarily on the unassigned contigs and cytologically near centromeres (Talbert et al. 2018; Chang et al. 2019). The 90U satellite corresponds to one of the nontranscribed ribosomal DNA (rDNA) spacer (NTS) subunits (Stage and Eickbush 2007). 90U repeats are adjacent to the 28S rDNA subunit and the 240-bp NTS repeat sequences, both on X-linked and unassigned contigs. We find a large 193XP locus in the pericentromeric heterochromatin adjacent to, but distinct from, the rDNA locus. In *D. simulans* and *D. mauritiana*, the 193XP loci span at least 48 kb. The 193XP locus is shared across the sim-complex but is absent in the outgroup species *D. melanogaster*, *D. erecta*, and *D. yakuba*, suggesting that it arose in the ancestor of the sim-complex. Consistent with our assemblies, we detect fluorescence in situ hybridization signal for 193XP only on the X pericentromere in the sim-complex (Supplemental Fig. S15).

We also find smaller satellite arrays in the euchromatin (Supplemental Table S9) as has been previously reported (Waring and Pollack 1987; DiBartolomeis et al. 1992; Kuhn et al. 2012; Gallach 2014). Satellites comprise only ~0.07% of bases in autosomal euchromatin, but they comprise 1% of X-linked euchromatin in *D. melanogaster* and *D. simulans*, up to 2.4% in *D. mauritiana*, and >3.4% in *D. sechellia* (Supplemental Table S9). The number in *D. sechellia* is a minimum estimate because its assembly contains six gaps in X-linked euchromatic satellite regions. The location, abundance, and composition of euchromatic satellites differ substantially between species. For example, a complex satellite called *Rsp-like* (Larracuent 2014) recently expanded in *D. simulans* and *D. mauritiana* and inserted into new X-linked euchromatic locations within existing arrays of another satellite called 1.688.

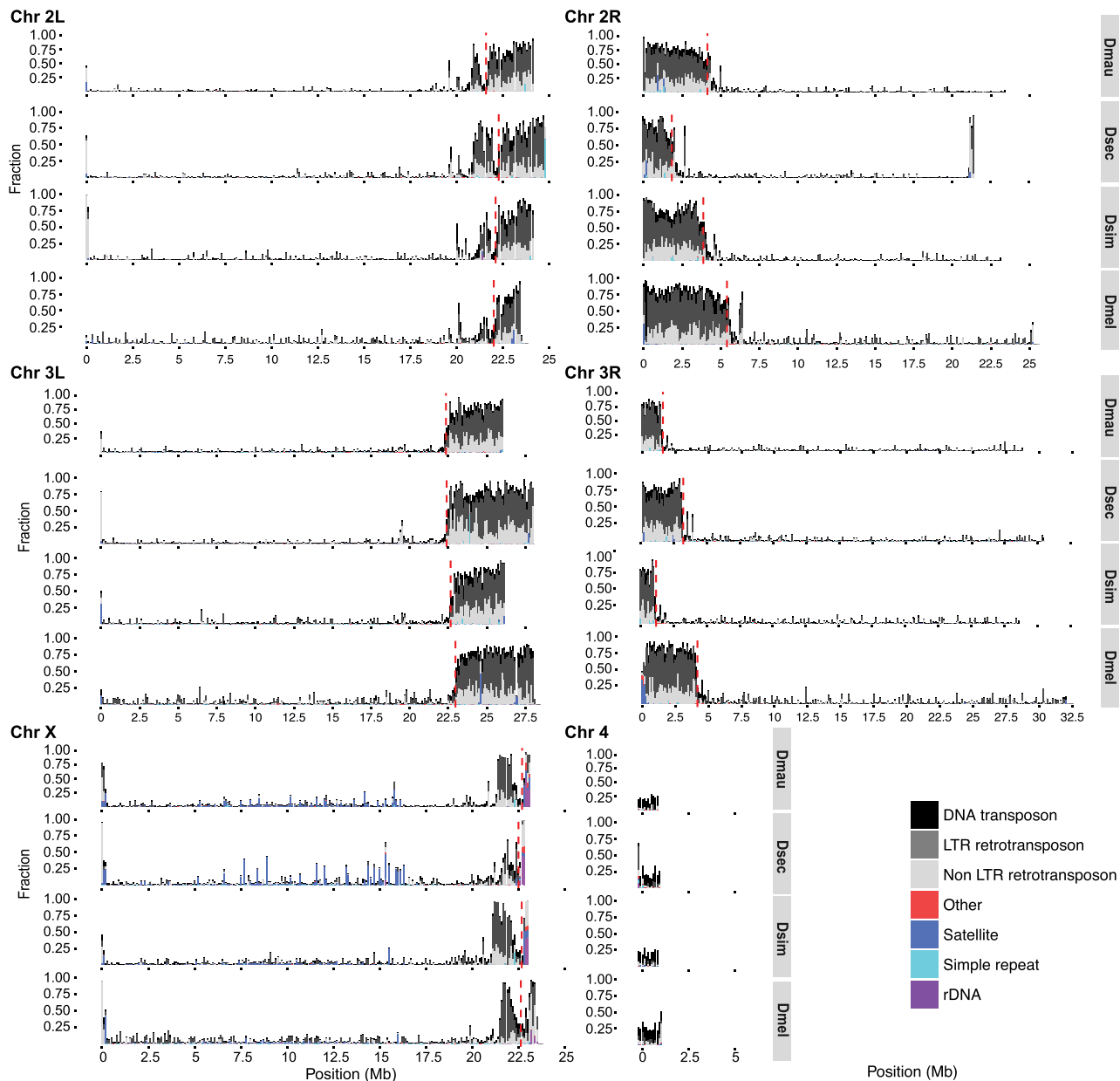


Figure 3. The repeat content across the chromosome arms in mel-complex species. We estimated the repeat content in the genome using RepeatMasker (Smit et al. 2013). Each bar represents the proportion of different repeat types in 100-kb windows. The red dashed vertical lines indicate the euchromatin–heterochromatin boundaries.

Large blocks of *1.688* (Lohe and Brutlag 1987) and *Rsp-like* (Larracuent 2014; Sproul et al. 2020) differ in abundance and location in the heterochromatin of all four species.

Transposable elements

We annotated euchromatic TEs across *D. melanogaster* and the three sim-complex species (see Methods). Unless otherwise noted, our results are based on comparisons of TE content (i.e., number of bases) rather than the number of TE insertions (i.e., number of events). We find that the sim-complex genomes host 67%–83% as much TE sequence as *D. melanogaster* (Fig.

4A). The major difference in TE composition among the four mel-complex species is the enrichment of LTR retrotransposons in *D. melanogaster* (Kaminker et al. 2002; Bergman and Bensasson 2007; Kofler et al. 2015), which carries 1.3–1.8 Mbp more LTR bases than the three sim-complex species (Fig. 4A,B). Both DNA and non-LTR transposon content in *D. melanogaster* are similar to those of the sim-complex species (Fig. 4A,B). Most TE bases (66%–72%) in the sim-complex are found in only one species' genome (Fig. 4C), implying that these sequences have resulted from recent transposon activity.

We also find that TE composition differs across the lineages that gave rise to these four species (Fig. 4D; Supplemental Fig.

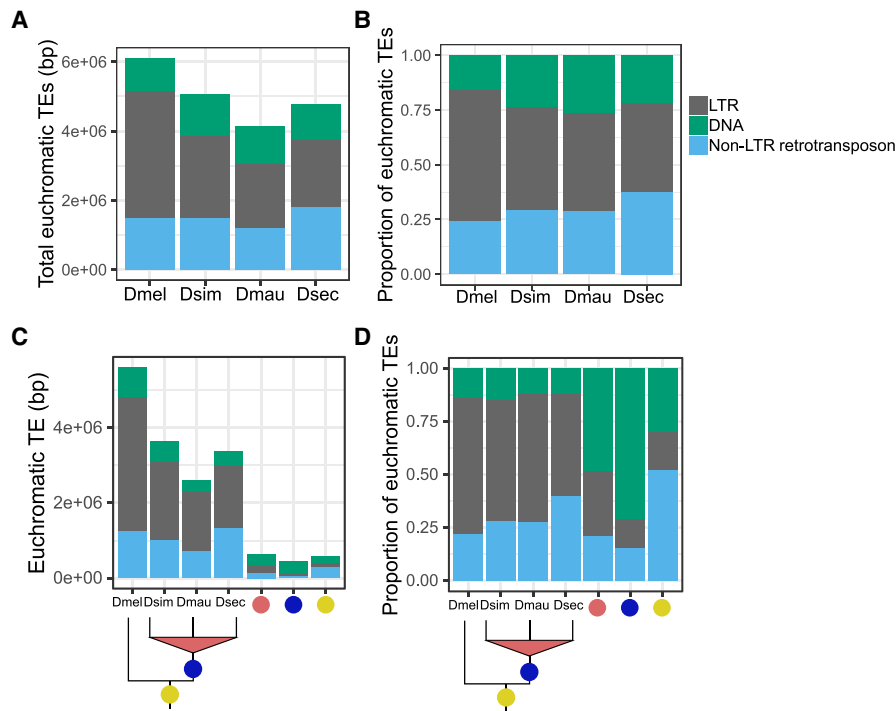


Figure 4. Euchromatic transposon sequence content in each species and their ancestral lineages in the mel-complex. The bars represent the absolute content (A,C) or relative proportion within each category (B,D) of TE bases owing to DNA and to LTR and non-LTR retrotransposon TEs. A and B show total TE content in each species. Panels C and D show the TE content confined to specific lineages. In panels C and D, the species names indicate TE sequence found only in that genome; the red circles indicate TE content found in two sim-complex species; the blue circles indicate TEs found in the sim-complex but not *D. melanogaster*; and the yellow circles indicate TE sequence found in all four mel-complex species.

S16). Within the syntenic TE content shared by all four mel-complex species, non-LTR retrotransposon sequence is the most prevalent (52%), followed by DNA transposons (30%) and LTR retrotransposons (18%). In contrast, orthologous TE sequences present in all three sim-complex species but not *D. melanogaster* are enriched in DNA transposons, which make up 71% of this orthologous sequence (Fig. 4D) despite being shorter than other TE classes (Supplemental Fig. S17). The *INE-1* element (also called *DINE-1* or *DNAREP1*) is a highly abundant DNA transposon in *Drosophila* (Quesneville et al. 2005; Yang and Barbash 2008) that has contributed to an abundance of shared *INE-1* elements fixed in mel-complex (Sackton et al. 2009). In our assemblies, *INE-1* makes up 46% of shared TE content in the lineage leading to the sim-complex, as well as a significant, but smaller proportion (13.7%) in the mel-complex lineage. The TE composition of spe-

cies-specific sequences is dominated by LTR elements (48%–57%) followed by non-LTR elements (27%–40%), with a smaller contribution of DNA elements (12%–16%) (Fig. 4D).

TE sequences can get incorporated into host genes (Lipatov et al. 2005). We find 0.8–1.6 Mb of TE sequence that overlaps with gene models in *D. melanogaster* and *D. simulans*. A small minority of young genic TEs (present only in *D. melanogaster*, only in *D. simulans*, or in the sim-complex but not *D. melanogaster*) are exonic (7%–18%) (Table 1). In contrast, half of the TE sequence present in all four mel-complex species is exonic (52%). This preponderance of exonic TE content in the mel-complex ancestor exceeds even the enrichment of non-LTR sequence across the whole genome (cf. Supplemental Fig. S18 and Fig. 4D).

Intron indel mutation patterns

We compared 21,860 introns in 6289 orthologous genes with conserved annotation positions in all four mel-complex species. We find that introns containing TE-derived sequences or complex satellites (“complex introns”) range from 530–850 bp longer in *D. melanogaster* (paired *t*-tests, all *P*-values < 0.001) (Supplemental Fig. S19), owing largely to longer intronic TEs (mean TE length = 4132 bp) compared with the sim-complex species (mean TE lengths of *D. simulans* = 2429 bp, *D. mauritiana* = 2253 bp, *D. sechellia* = 2287 bp) (Supplemental Fig. S20). Among sim-complex species, *D. sechellia* has the longest complex introns in heterochromatin (both paired *t*-tests *P*-values < 0.05) but not in euchromatin (paired *t*-tests *P*-value > 0.09) (Supplemental Table S10; Supplemental Fig. S19). Similar to the complex introns, introns without transposons or complex satellite sequences (“simple introns”) are significantly longer in *D. melanogaster* than the sim-complex species (paired *t*-tests, all *P*-values < 1×10^{-7}) (Supplemental Fig. S19; Supplemental Table S10), but the mean length difference is < 3 bp (Supplemental Table S10). Consistent with a previous report (Presgraves 2006), we infer that this difference is partly owing to an insertion bias in *D. melanogaster* (see Supplemental Information, methods and analyses).

Table 1. TE bases in *D. melanogaster*, *D. simulans*, the ancestral lineages of the sim-complex species (mau-sec-sim), and the mel-complex species (mel-mau-sec-sim) in 6984 conserved genes

Lineage	Genic (bp)	Exonic (bp; % of genic)	Intronic (bp; % of genic)
<i>D. melanogaster</i>	1,621,900	292,080 (18.0%)	1,329,820 (82%)
<i>D. simulans</i>	806,226	140,174 (17.3%)	666,052 (82.7%)
mau-sec-sim	88,202	5906 (6.7%)	82,296 (93.7%)
mel-mau-sec-sim	185,217	96,849 (52.3%)	88,368 (47.7%)

Verification of transcript expression in the sim-complex is based on Iso-Seq from *D. simulans* (Nouhaud 2018), so species-specific classifications are not available for *D. mauritiana* or *D. sechellia*.

Tandem duplication

We found 97 euchromatic tandem duplications shared by all three sim-complex species but absent from *D. melanogaster* (Supplemental Table S11). Among these, at most 11 overlapped with duplications observed in the outgroup *D. yakuba*, suggesting that at least 86 duplications originated during the ~2.5 million years in the ancestral lineage of the sim-complex since diverging from *D. melanogaster*. Of these duplications, 72% (62/86) overlap exons, 37% (32/86) overlap complete protein-coding sequence, and 15% (13/86) overlap one or more full-length *D. melanogaster* genes. In total, 32 complete coding sequences were duplicated, or 12.8 new genes per million years. Similar to the polymorphic duplicates in *D. simulans* (Rogers et al. 2014), tandem duplications fixed in the sim-complex ancestral lineage are strongly enriched on the X Chromosome relative to the autosomes (43/86; P -value $< 1 \times 10^{-10}$, proportion test against X-linked genes as a proportion of all genes, or 0.158). As a result, the X Chromosome carries both an excess of duplicates spanning full coding sequences (15 X-linked, 17 autosomal; P -value = 4.7×10^{-6} , proportion test against the proportion of X-linked genes) as well as full transcripts (six X-linked, seven autosomal; P -value = 2.8×10^{-3} , proportion test against the proportion of X-linked genes).

Several duplication events include genes associated with divergence of important phenotypes, including spermatogenesis (*nsr*) (Ding et al. 2010), meiosis (*cona*), odorant binding (*obp18a*), chromosome organization (*HP1D3csd*), and behavior (*RhoGAP18B*) (Rothenfluh et al. 2006). Many are absent in the previous assemblies of the sim-complex species. For example, we discovered a new X-linked 3324-bp duplication that copied the genes *maternal haploid (mh)* and *Alg14*. Analysis of *D. mauritiana* and *D. simulans* RNA-seq reads from our strains and Iso-Seq reads from another *D. simulans* strain (Nouhaud 2018) suggests that the distal copy (*mh-d*) produces a shortened transcript and protein compared with *mh-p* and the ancestral *mh* (Fig. 5A; Supplemental Fig. S21, S22). *mh-p* has female-biased expression in *D. simulans*, as does *mh* in *D. melanogaster*, where it has an essential maternal effect in zygotic cell division (Loppin et al. 2001; Delabaere et al. 2014). In contrast, *mh-d* shows testis-biased expression (Fig. 5B; Supplemental Fig. S21), suggesting that *mh-d* may have acquired a male-specific function in the sim-complex species.

We also uncovered a 4654-bp tandem duplication located entirely in an inverted segment of the pericentric heterochromatin on the sim-complex X Chromosome that partially copied the gene *suppressor of forked (su(f))* (Supplemental Fig. S23). This duplicate is absent in the previous *D. mauritiana* assembly (Garrigan et al. 2014) and the reference genomes of *D. simulans* (r2.02) and *D. sechellia* (r1.3). The proximal *su(f)* copy is missing the first 12 co-

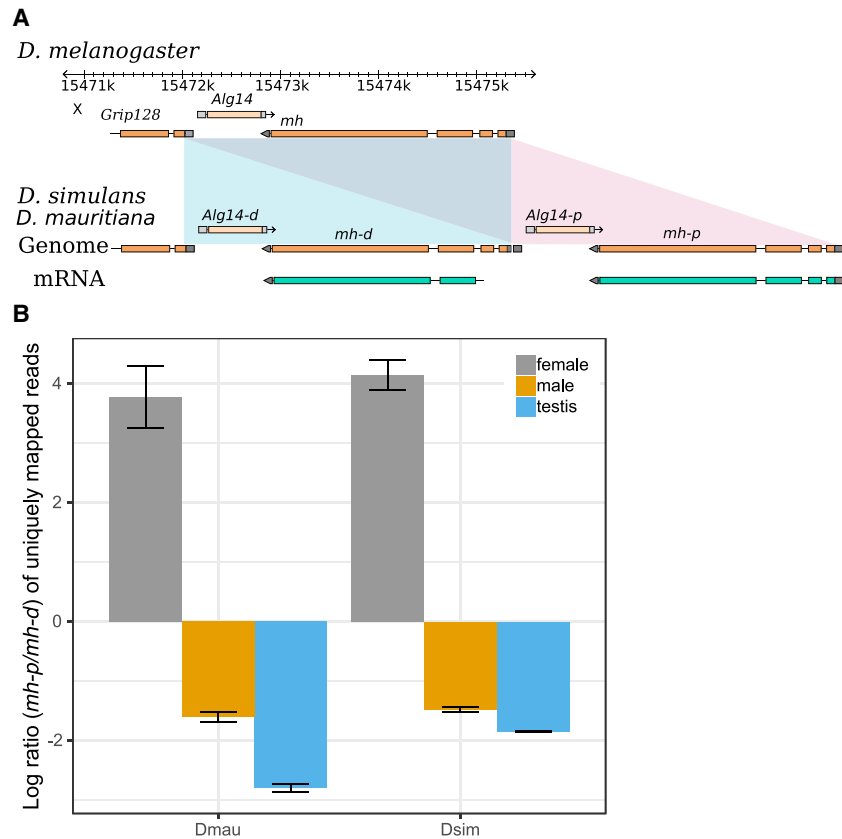


Figure 5. The expression divergence of *maternal haploid (mh)* duplications in the sim-complex species. (A) The sim-complex shares a tandem duplication of *mh* and *Alg14* genes. The expression of both *mh* copies is supported by Iso-Seq and Illumina transcriptome data. (B) The proximal copy of *mh* (*mh-p*) is primarily expressed in females, and the distal copy (*mh-d*) shows testis-biased expression in both *D. mauritiana* and *D. simulans*.

ditions but retains the rest of the ORF of the parental *su(f)* coding sequence, including the stop codon (Supplemental Fig. S23).

Evolution of tRNA clusters

Nuclear tRNAs are distributed both individually and in clusters containing identical copies coding for the same amino acids (isoacceptor tRNAs) and interspersed with those coding for different amino acids (alloacceptor tRNAs). Previous analyses found a smaller complement of tRNAs in *D. simulans* than in *D. melanogaster* (*Drosophila* 12 Genomes Consortium 2007), although it could have been owing to a difference in assembly quality (*Drosophila* 12 Genomes Consortium 2007; Rogers et al. 2010; Velandia-Huerto et al. 2016). We found genome-wide tRNA counts to be similar between the species, ranging from 295 in *D. melanogaster* to 303 copies in *D. sechellia* (Supplemental Fig. S24; Supplemental Table S12).

Our count of tRNAs in *D. simulans* (300 tRNAs) is substantially higher than previously reported using an older assembly (268 and 255 tRNAs) (Rogers et al. 2010; Velandia-Huerto et al. 2016, respectively), suggesting that the high rates of tRNA loss reported previously were owing to assembly errors.

We identified putative tRNA orthologs using alignments encompassing tRNAs and identified syntenic blocks of tRNAs that differed in copy number, identity (isotype), anticodon, and

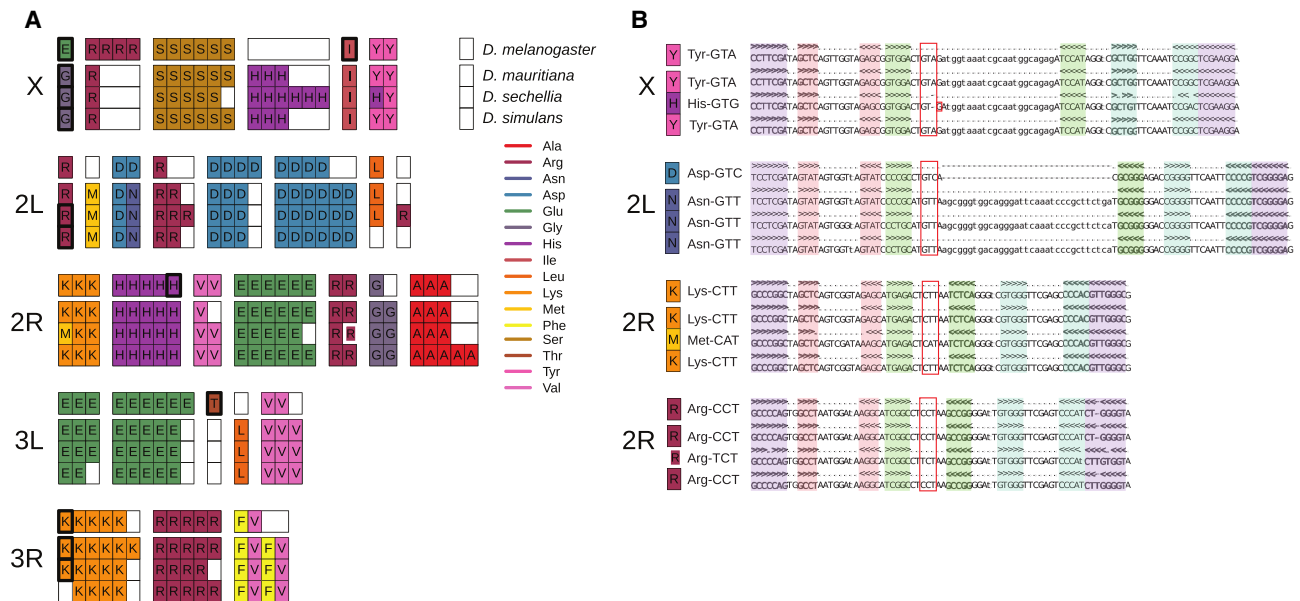


Figure 6. Nuclear tRNA sequences in the four mel-complex species. (A) The subset of all nuclear tRNAs that differ in copy-number, isotype identity, or anticodon sequence between four mel-complex species. Each box represents an individual tRNA gene copy located within a larger syntenic cluster of tRNAs (grouped together as colored columns). Thick black outlines show tRNAs predicted to be pseudogenes. The thick white outline shows an arginine tRNA on Chromosome 2R predicted to use a different anticodon. (B) Secondary structure alignments of orthologous nuclear tRNAs that show anticodon shifts. The tRNA anticodon (red box), acceptor stem (purple), D arm (red), anticodon arm (green), and T arm (blue) are highlighted in the alignments. See Supplemental Figure S24 for relative position on the chromosomes.

pseudogene designations (Fig. 6A,B). To confirm gains or losses, we used a BLAST-based approach, similar to methods used by Rogers et al. (2010), to identify regions flanking orthologous tRNA clusters. We identified four tRNA anticodon shifts, including one iso-acceptor and three alloacceptor shifts (Fig. 6B), consistent with previous reports (Rogers et al. 2010; Rogers and Griffiths-Jones 2014; Velandia-Huerto et al. 2016). We did not detect a previously identified alloacceptor shift (Met CAT>Thr CGT) (Rogers and Griffiths-Jones 2014; Velandia-Huerto et al. 2016), which could be because of allelic variation within *D. simulans*. In each case, the derived tRNA sequence was otherwise similar to and retained the predicted structure of the ancestral tRNA, suggesting that the alloacceptor shifts cause the aminoacyl tRNA synthetase (aaRS) to charge the affected tRNAs with the amino acid cognate to the ancestral tRNA, integrating the wrong amino acid during translation.

Y Chromosome evolution

We identified Y-linked contigs in the sim-complex genomes using *D. melanogaster* Y-linked genes as queries. Y-linked contigs were short (<1 Mb) and lacked some homologous exons present in raw reads (e.g., exons 8–10 of *kl-3* and exons 6–8 of *kl-5*) (Supplemental Table S13; see also Krsticevic et al. 2015; Chang and Larracuente 2019), highlighting the challenges of assembling Y Chromosomes even with long-read sequencing. We recovered 66, 58, and 64 of 83 *D. melanogaster* Y-linked exons (70%–80%) (Supplemental Table S13) in *D. mauritiana*, *D. simulans*, and *D. sechellia*, respectively. A previous study found a duplication involving the Y-linked *kl-2* gene in *D. simulans* (Kopp et al. 2006). We find that all known Y-linked genes, except *Ppr-Y*, exist in multiple copies in at least one of the sim-complex assemblies, and one exon of *Ppr-Y* appears duplicated in *D. mauritiana* raw long reads. Most duplication events

correspond to partial tandem duplications (all but *ARY*, *Pp1-Y1*, and *Pp1-Y2*). We validated one duplicated exon from each of 10 Y-linked genes using PCR resequencing (except *Pp1-Y1*, which lacked mutations differentiating copies) (Supplemental Table S13, S14). Some duplicated exons (e.g., *kl-5* exons 9 and 10) are shared among sim-complex species, whereas other exons vary in copy number among species. For example, *ARY* is single copy in *D. melanogaster* and *D. simulans* but present in more than three copies in *D. sechellia* and *D. mauritiana*.

We identified 41 duplications from other chromosomes to the Y Chromosome only in the sim-complex species (Supplemental Table S15), including 30 duplications not previously identified (Tobler et al. 2017). Among the 41 Y-linked duplications, 22 are shared by at least two sim-complex species and likely originated in the ancestor of the sim-complex. We verified putative Y-linked duplicates with PCR, confirming male-specificity for 16 of 17 of tested duplications (Supplemental Tables S14, S15). We found that the Y Chromosomes of sim-complex species share an insertion derived from mtDNA that is absent in *D. melanogaster*.

Discussion

Here we uncover novel structural variation in both euchromatin and highly repetitive pericentromeric regions of the *D. simulans* species complex. This variation is substantial: ~15% of sim-complex genomes are not 1:1 orthologous with *D. melanogaster*, more than twice the number of nucleotide substitutions between these genomes (Begun et al. 2007). We find most rearrangements in heterochromatic genomic regions (Jagannathan et al. 2017; Sproul et al. 2020) likely influenced by both the density of repetitive DNA and the scarcity of genes. The former renders DNA repair mechanisms mutagenic, creating rearrangements, whereas the latter reduces selection against rearrangements in these regions. Such

heterochromatic rearrangements may play a role in speciation, as many factors linked to genetic incompatibilities between species are located in pericentromeric heterochromatin (Bayes and Malik 2009; Cattani and Presgraves 2009; Ferree and Barbash 2009).

We also discovered 62 tandem duplications present only in the sim-complex genomes that duplicate one or more protein-coding exons. Such mutations frequently contribute to adaptation, functional innovation, and genetic incompatibilities (Lynch and Force 2000; Long et al. 2003; Ting et al. 2004; Arguello et al. 2006; Katju and Lynch 2006; Tao et al. 2007b; Zhou et al. 2008; Chakraborty and Fry 2015; Helleu et al. 2016; Eickbush et al. 2019). In the branch leading to the sim-complex, the rate of new gene acquisition is roughly one new gene every 78,000 yr for full duplicates (about 12.8 duplicates per Myr) or one new gene per 40,000 yr for partial gene duplicates (about 24.8 duplicates per Myr). The lower bound of these rates (1×10^{-9} to 2×10^{-9} new genes/gene/year) is consistent with previous estimates over a different timescale (Osada and Innan 2008). These estimates suggest that the rate of new gene acquisition per single copy gene is similar to the per nucleotide neutral mutation rate (Keightley et al. 2014). The proportion of exonic duplicates fixed in the sim-complex branch is greater than the proportion of polymorphic exonic duplicates in *D. simulans* (0.72 vs. 0.408, proportion test, P -value = 3.41×10^{-9}) (Rogers et al. 2014), whereas the proportion of intergenic (i.e., putatively nonfunctional) duplicates shows the opposite pattern (0.28 vs. 0.43, proportion test, P -value = 0.0029). This suggests that either the exonic duplicates accumulated under positive selection in the sim-complex ancestral lineage or the polymorphism data, which are based on short reads, are missing duplicates. Further study with polymorphism data from highly contiguous *D. simulans* genome assemblies will resolve this puzzle.

These *Drosophila* genomes differ in TE content and composition, likely owing to historical and ongoing differences in TE activity, natural selection, and host genome repression. Approximately 75%–80% of TE content in all four genomes is because of species-specific insertions (Fig. 4), which are likely polymorphic within species (Chakraborty et al. 2018). This is consistent with most TE content resulting from recent activity (*Drosophila* 12 Genomes Consortium 2007; Lerat et al. 2011; Kofler et al. 2015; Bargues and Lerat 2017). Non-LTR retrotransposons comprise the majority (52%) of the old TEs found in all four mel-complex species, whereas DNA transposons comprise most (71%) of the younger fixed TE sequences found only in the sim-complex species. The widespread *INE-1* DNA element (Quesneville et al. 2005; Yang and Barbash 2008; Sackton et al. 2009) is far more prevalent in the sim-complex ancestor than in the mel-complex ancestor, suggesting a burst of *INE-1* activity in the sim-complex after diverging from *D. melanogaster*. On the other hand, *D. melanogaster*'s genome is enriched for LTR elements owing to recent TE activity in this lineage (Bowen and McDonald 2001; Bergman and Bensasson 2007; Kofler et al. 2015). These LTRs have increased the size of *D. melanogaster*'s genome through both intergenic and intragenic insertions, so that euchromatic introns containing repetitive DNA are ~10% longer in *D. melanogaster* than sim-complex species, (Supplemental Information, methods and analyses). However, although the sim-complex does harbor less TE content than *D. melanogaster* (Fig. 4A; *Drosophila* 12 Genomes Consortium 2007), we observe only ~17% less total TE sequence in *D. simulans* than in *D. melanogaster*, which is substantially lower than previously reported (Young and Schwartz 1981; Dowsett and Young 1982; Nuzhdin 1995; Vieira et al. 1999; Vieira and Biémont 2004; *Drosophila* 12 Genomes Consortium 2007).

Intron size evolution may also be modulated by differences in insertion and deletion mutations (Petrov et al. 1996; Petrov and Hartl 1998; Blumenstiel et al. 2002), recombination rates (True et al. 1996; Brand et al. 2018), effective population sizes (Kofler et al. 2012), or variation in constraint mediated by the presence of conserved noncoding elements (Manee et al. 2018). Further study is needed to determine which factors contribute to the differences between sim-complex genomes. For example, among the sim-complex species, *D. sechellia* has the longest complex introns in heterochromatin, but not in euchromatin (Supplemental Table S10), which could be a result of both low recombination rates in heterochromatin and the small effective population size of this species (Kliman et al. 2000; McBride 2007; Singh et al. 2007). A small effective population size in *D. sechellia* might also lead to the enrichment of tRNA anticodon shifts (75% of all observed) and expansion of euchromatic satellites.

TE activity is deleterious (Petrov et al. 2011; Cridland et al. 2013; Chakraborty et al. 2019): Transposition disrupts genes and other functional elements (e.g., Supplemental Fig. S25; Cooley et al. 1988); TE sequences can act as ectopic regulatory elements (Feschotte 2008) and provide templates for ectopic recombination (Montgomery et al. 1987; Miyashita and Langley 1988). Like other eukaryotes, *Drosophila* has evolved host defenses against TE proliferation (Aravin et al. 2007; Brennecke et al. 2007; Chung et al. 2008; Kelleher et al. 2018). Interspecific differences in these host defenses may contribute to the TE abundance differences between the sim-complex and *D. melanogaster*. TE insertions also alter local chromatin state in *Drosophila*, which can spread and suppress the expression of adjacent genes, with potentially deleterious consequences (Lee and Karpen 2017). Heterochromatin proteins are expressed at higher levels in *D. simulans* than *D. melanogaster*, which may cause heterochromatin to spread further from TEs into nearby regions in *D. simulans* (Lee and Karpen 2017). Thus, selection to eliminate euchromatic TE insertions may be stronger in *D. simulans* than in *D. melanogaster*, contributing to the excess of TEs in the latter. We identified a recent duplication of *su(f)*, a suppressor of *Gypsy* LTR retrotransposon expression, in all sim-complex species (Parkhurst and Corces 1986; Mazo et al. 1989). The extra copy could contribute to the lower activity and prevalence of LTR elements in the sim-complex species compared with *D. melanogaster* (Fig. 4).

Sex chromosomes play a special role in the evolution of post-zygotic hybrid incompatibilities (Coyne and Orr 1989). We find that euchromatic duplications, deletions, and inversions are enriched on the X Chromosome (Supplemental Table S11): 90% of all rearrangements between sim-complex genomes are X-linked (Supplemental Table S8). We also report an enrichment (approximately 15- to 50-fold) of X-linked satellite sequences, exceeding even previous reports (approximately 7.5-fold) (Garrigan et al. 2014). Ectopic exchange between repeats during DNA repair can create genomic rearrangements. X-linked euchromatic satellites may contribute to the enrichment of rearrangements on this chromosome (Fig. 2A; Supplemental Table S9; Sproul et al. 2020). It remains unclear whether these rearrangements contribute to the enrichment of hybrid incompatibility factors on the X Chromosomes within the sim-complex (Tao and Hartl 2003; Masly and Presgraves 2007). The sim-complex genomes also contain a duplication of *mh*, whose protein product interacts with the X-linked heterochromatic satellite called *359-bp*—a member of the *1.688 gm/cm³* satellites, to maintain genome stability during embryogenesis (Loppin et al. 2001; Delabaere et al. 2014; Tang et al. 2017). The derived copy of *mh* produces a shorter transcript

than the ancestral copy, has male-biased expression, and likely binds to 359-bp, given the similarity between the ancestral and derived proteins (Supplemental Fig. S21). We speculate that the duplicated *mh* may play a role in the male germline regulating 359-bp-related satellites that have proliferated across the sim-complex species X Chromosomes (Jagannathan et al. 2017; Sproul et al. 2020).

Despite harboring few genes, the *Drosophila* Y Chromosome contributes to hybrid incompatibilities and affects phenotypes including longevity, immunity (Case et al. 2015; Kutch and Fedorka 2015; Araripe et al. 2016; Brown et al. 2020), meiotic drive (Voelker 1972; Atlan et al. 1997; Unckless et al. 2015), male fitness (Chipindale and Rice 2001), and gene expression across the genome (Lemos et al. 2010; Branco et al. 2013). We discovered extensive divergence between mel-complex species in the genic content of Y Chromosomes resulting from rampant inter- and intrachromosomal duplication. Y-linked gene content in *Drosophila* is shaped by gene duplication from the autosomes (Kopp et al. 2006; Koerich et al. 2008; Carvalho et al. 2015; Ellison and Bachtrog 2019). We detect 41 duplications from the other chromosomes to sim-complex Y Chromosomes. We also discovered that nearly all Y-linked genes are duplicated in at least one species. This amplification of Y-linked genes appears to be a common feature of *Drosophila* Y Chromosomes and may reflect a strategy to compensate for the heterochromatic environment or ongoing genetic conflict with the X Chromosome (Kopp et al. 2006; Koerich et al. 2008; Carvalho et al. 2015; Ellison and Bachtrog 2019).

The structural divergence between these species extends to the endosymbionts they carry. We uncovered extensive structural evolution in *Wolbachia* genomes between *w*Mau and the corresponding *D. simulans* *Wolbachia* strains (Supplemental Fig. S8A–C). Further study is necessary to understand whether such variants affect important phenotypes like titer and transmission (Serbus and Sullivan 2007; Meany et al. 2019), virulence (Chrostek and Teixeira 2018), fitness (Turelli and Hoffmann 1995; Kriesner et al. 2013), *Wolbachia* frequency variation (Kriesner et al. 2016; Cooper et al. 2017), or cytoplasmic incompatibility (Hoffmann and Turelli 1997).

Previous assemblies were biased toward unique sequences, neglecting repetitive regions (*Drosophila* 12 Genomes Consortium 2007; Bhutkar et al. 2008; Garrigan et al. 2012; Hu et al. 2013). However, these regions harbor extensive hidden genetic variation relevant to genome evolution and organismal phenotypes (Khost et al. 2017; Chakraborty et al. 2018, 2020; Stein et al. 2018; Chaisson et al. 2019; Chang and Larracuent 2019; Stitzer et al. 2019; Miga et al. 2020). Understanding the evolution of these rapidly diverging repetitive, complex genomic regions and their effects on adaptation and species differentiation requires a direct comparison between closely related species. Here we show that the genomes of these four *Drosophila* species have diverged substantially in the regions that have been previously recalcitrant to assembly. Future studies of interspecific variation in genome structure will shed light on the dynamics of genome evolution underlying speciation and species diversification.

Methods

Data collection

Unless otherwise stated, we use the following strains: *D. mauritiana* (*w*12), *D. simulans* (*w*^{XD1}), and *D. sechellia* (Rob3c/Tucson 14021-0248.25) (Garrigan et al. 2012; Meiklejohn et al. 2018). We extract-

ed gDNA following Chakraborty et al. (2016). The standard 20-kb library protocol was performed at the UCI genomics core using the P6-C4 chemistry on Pacific Biosciences (PacBio) RS II.

To collect RNA sequencing, flies from the sim-complex species were reared at room temperature on a standard cornmeal-molasses medium. We collected 20–30 3- to 5-d-old virgin males and females and dissected testes from at least 100 males. For *D. simulans* and *D. mauritiana*, total RNA was extracted using TRIzol (Invitrogen) and phase-lock gel tubes (Thermo Fisher Scientific). Sequencing libraries generated by Illumina TruSeq stranded mRNA kit were sequenced at the University of Minnesota Genomics Center. For *D. sechellia*, we isolated total RNA using the RNeasy plus kit (Qiagen) and constructed libraries using TruSeq RNA sample preparation kit V2 (Illumina) with oligo(dT) selection (data available at the NCBI BioProject database [https://www.ncbi.nlm.nih.gov/bioproject/] under accession number PRJNA541548).

Genome assembly

Nuclear genome assembly

We assembled the nuclear genomes of the sim-complex species de novo following the previously described approaches for assembly and polishing (Supplemental Fig. S26; Chakraborty et al. 2016). To ascertain putative misassemblies, we identified orthologs of all *D. melanogaster* heterochromatic genes using BLAST and examined their gene structure. Because interchromosomal rearrangements in the mel-complex species have not been attested in the cytology literature (Bhutkar et al. 2008), we flagged as potential misassemblies the contigs with genes that translocated between chromosome arms or that appeared on more than two contigs. We combined this evidence with empirical data to manually fix 10 misassemblies (Supplemental Table S16; Supplemental Fig. S27). This includes independent assemblies of mitochondrial and *Wolbachia* genomes, as the original contigs yielded misassembly sizes of these circular genomes.

Mitochondrial genome assembly

We extracted raw reads mapping to an existing partial mitochondrial genome using BLASR (Chaisson and Tesler 2012; https://github.com/mahulchak/mito-finder). We selected the longest read exceeding a length cutoff of 18 kb (the mitochondrial genome is ~19 kb) and trimmed the redundant sequences resulting from multiple polymerase passes through the SMRTbell template. Trimmed reads were polished twice with Quiver (Chin et al. 2013) to generate a consensus of all mitochondrial reads.

Wolbachia genome assembly

We took advantage of the fact that endosymbionts are cosequenced with their hosts in shotgun sequencing data to assemble complete *Wolbachia* genomes from our PacBio data (Faddeeva-Vakhrusheva et al. 2017; Basting and Bergman 2019; Kampfraath et al. 2019). We identified a complete *Wolbachia* genome in *D. mauritiana* from the Canu assembly. For *D. sechellia*, we collected all reads mapping to two reference *Wolbachia* genomes (CP003884.1 and CP003883) using BLASR v5.1 (Chaisson and Tesler 2012) with parameters (--clipping soft --bestn 1 --minPctIdentity 0.70). We assembled these reads using Canu v1.3 with the parameters (genomeSize=3m) (Koren et al. 2017). No *D. simulans* reads were mapped to the *Wolbachia* genomes.

Assembly validation and quality control

We evaluated long-read coverage to identify assembly errors and validate copy number variants. We mapped raw long reads to assemblies using *BLASR* (version 1.3.1.142244; parameters: `-bestn 1 -sam`) (Chaisson and Tesler 2012) or *minimap2* (2-2.8 parameters: `-ax map-pb`) (Li 2016). We calculated long-read coverage across the contigs using the *SAMtools* *mpileup* and *depth* (`-Q 10 -aa`) commands. To validate CNVs, we chose 20 random CNVs for each species and inspected long-read coverage across the regions containing CNVs following (Chakraborty et al. 2018). The presence of at least three long reads spanning the entire CNV was classified as evidence supporting the variant.

We used the script in Masurca v3.2.1 (Zimin et al. 2013) to identify redundant sequences in our assemblies. We designated contigs as residual heterozygosity candidates (those >40 kb require >90% identity, and those between 10 and 40 kb require >95% identity to the longest contigs). To detect microbial contamination in our assemblies (Supplemental Table S7), we used *BLAST+* v2.6.0 (Altschul et al. 1990) with *BlobTools* (0.9.19.4) (Laetsch and Blaxter 2017) to search the NCBI Nucleotide database (parameters “`-task megablast -max_target_seqs 1 -max_hsp 1 -evalue 1 × 10-25`”) and calculated the Illumina coverage of all contigs for *D. mauritiana*, *D. simulans*, and *D. sechellia*, respectively (Supplemental Table S17; Supplemental Fig. S28).

We applied the method of Koren et al. (2018) to the polished, prescaffolded assemblies to estimate base level error rates from the concordance between Illumina reads and an assembly of the same strain (i.e., QV). We calculated BUSCOs in our assemblies with *BUSCO* v3.0.2 against the Diptera database (Waterhouse et al. 2017). Some duplicated BUSCOs in *D. simulans* remained because of persistent alternate haplotigs. We inspected these 71 duplicate BUSCOs, identifying 58 with one member on Muller element contigs and the others on smaller, putative alternate haplotigs. BUSCO metrics were recalculated without these unplaced contigs (Supplemental Table S5). We also applied *QUAST* v5.0.2 (Mikheenko et al. 2018) to evaluate the quality of assemblies based on the mapping status of Illumina data. For *D. simulans* and *D. sechellia*, we used independently generated male and female reads (Wei et al. 2018) to avoid the ascertainment bias owing to the Illumina reads used in polishing our assemblies (Supplemental Table S17). For *D. mauritiana*, we used the female Illumina reads for both our assembly and the previous assemblies (Garrigan et al. 2014).

Scaffolding

We scaffolded the assemblies with *mscaffolder* (<https://github.com/mahulchak/mscaffolder>) following the method of Chakraborty et al. (2018) using *D. melanogaster* as the reference. Scaffolded contigs were joined with 100 Ns, and unscaffolded contigs were prefixed with “U.”

Annotation

Transcript annotation

We mapped transcripts and translated sequences from *D. melanogaster* (r6.14) to each assembly using *MAKER2* (v2.31.9) (Holt and Yandell 2011). We also generated RNA-seq from whole females, whole males, and testes from the sim-complex species. We mapped this data (see details in Supplemental Table S18) using *HISAT2* 1.0 with the *MAKER2* annotation and then used *StringTie* 1.3.4d to generate consensus annotations (Pertea et al. 2016). We further annotated putative duplicated genes in *D. simulans* using Iso-Seq data from Nouhaud (2018). We applied the *IsoSeq3* pipeline (v3.1.2) to correct and polish the raw reads and then generated

full-length cDNA sequences (Gordon et al. 2015). Polished cDNA sequences were mapped to the assembly using *minimap2* (r2.16) (Li 2016) with the parameters “`-t 24 -ax splice -uf --secondary=no -C5`.” We then used *cdna-cupcake* (v10.0.1 with the parameter “`--dun-merge-5-shorter`”) (https://github.com/Magdoll/cDNA_Cupcake) to cluster the isoforms in the cDNA alignment and transfer it to the annotation. We used *BLAST* (`-evalue 1 × 10-10`) (Altschul et al. 1990) homology to assign the predicted transcripts to *D. melanogaster* transcript sequences. To identify conserved introns, we kept isoforms with the same numbers of exons and only used introns flanked by exons of similar size (within 10% length difference) in each species. To compare intron sizes between species, we used the longest isoform from each gene. We also annotated 61 introns from six genes with large introns (>8 kb) based on *BLAST* results.

Large structural variant detection

To identify large-scale synteny, we created whole-genome alignments with the *Mauve* aligner (build 2015-2-13) using the *progressiveMauve* algorithm (Darling et al. 2010) with the default parameters: default seed weight, determine LCBs (minimum weight = default), full alignment with iterative refinement. We plotted gene density based on *Dm6* annotations in *D. melanogaster* was plotted using *Karyoploter* (Gel and Serra 2017).

Annotation of repetitive elements

We annotated new complex satellites using *Tandem Repeat Finder* and annotated novel TEs using the *REPET* TE annotation package (Supplemental Fig. 29A,B; Flutre et al. 2011). We removed complex satellite annotations from the *Drosophila* Repbase release (20150807), and combined the rest of the library with our newly annotated satellites and TEs. We then updated repeat classifications (Supplemental Fig. 29C) and used the resulting library (Supplemental File S1) to annotate the three sim-complex species and the *D. melanogaster* reference with *RepeatMasker* v4.0.5 (Supplemental Fig. 29; Smit et al. 2013).

We calculated the proportion of each repeat family and the proportion of TEs that are DNA transposons, non-LTR, and LTR retrotransposons in 100-kb windows across the scaffolds containing major chromosome arms. We determined approximate euchromatin/heterochromatin boundaries in the major scaffolds based on boundaries from *D. melanogaster* (Hoskins et al. 2015) in each sim-complex assembly. We considered Chromosome 4 and all unassigned contigs to be heterochromatin. TE sequence annotations in our *D. simulans* assembly were called exonic when they fell inside the alignment between the Iso-Seq transcript and the genome.

tRNA annotation and analysis

We used *tRNAscan-SE* v1.4 (options: `-H`) (Lowe and Eddy 1997) to annotate tRNAs and predict secondary structures in the *D. melanogaster* reference (r6.09) and in sim-complex assemblies. We sorted tRNAs by position and represented them as peptide sequences based on the predicted tRNA isotype that we aligned using *MUSCLE* v3.8.31 (Edgar 2004). We inspected these coarse alignments of tRNA positions for each chromosome (X, 2L, 2R, 3L, 3R) using conservation of gene order, strand orientation, inter-tRNAs distances, anticodon sequence, and intron positions to identify positional tRNA orthologs within syntenic clusters (see Supplemental Information, methods and analyses). We also used a *BLAST*-based orthology discovery method—similar to methods described by Rogers et al. (2010)—to map tRNAs from *D. mauritiana*, *D. sechellia*, or *D. simulans* that did not share positional

orthologs with tRNAs in *D. melanogaster* (see Supplemental Information, methods and analyses).

Genomewide SV annotation

We aligned each member of the sim-complex to *D. melanogaster* (Hoskins et al. 2015) using MUMmer 4.0 (NUCmer -maxmatch) (Marçais et al. 2018) and LASTZ (Harris 2007). MUMmer alignments were processed using SVMU v0.3 (structural variants from MUMmer) (Chakraborty et al. 2018, 2019; <https://github.com/mahulchak/svmu> commit 9a20a2d) to annotate the SVs as duplicates originating in either the sim-complex or *D. melanogaster*. We added duplications that MUMmer failed to recover using an approach based on LASTZ alignments (Schwartz et al. 2003) and UCSC Genome Browser alignment chaining. The LASTZ/axtChain workflow is available at GitHub (https://github.com/yiliao1022/LASTZ_SV_pipeline; Kent et al. 2003). Additional details are provided in the Supplemental Information (see supplemental section “SV annotation, validation and analysis”).

Shared TE analysis

We limited the shared TE analysis to euchromatic regions. To identify TEs shared between species, we performed all pairwise alignments of the sim-complex species to each other and to *D. melanogaster* using NUCmer -maxmatch -g 1000 in MUMmer v4. We extracted syntenic regions from alignment with svmu 0.3 and validated these regions by inspecting the dotplots (Supplemental Fig. S30). To identify TE sequences completely contained with syntenic regions between species pairs, we used BEDTools (BEDTools -u -f 1.0 -a te.bed -b cm.eu.txt) (Quinlan and Hall 2010). We identified TEs shared among all four mel-complex species using the *D. mauritiana* genome as the reference. TEs shared between *D. mauritiana*–*D. sechellia* (A) and *D. mauritiana*–*D. simulans* species pairs (B) were inferred to be derived from either the sim-complex or mel-complex ancestral lineages (Fig. 4), whereas TEs shared between A, B, and *D. mauritiana*–*D. melanogaster* pairs were inferred to be derived from the TEs fixed only in the mel-complex ancestral lineage (BEDTools intersect -u -a te.simclade.bed -b te.dmau-dmel.bed). We report differences in the abundance of existing TE families within these genomes and make no inferences that TEs are restricted to or missing from any subset of these four species.

Y Chromosome analyses

We used BLAST to identify the orthologs of all known *D. melanogaster* Y-linked genes in the sim-complex assemblies (Altschul et al. 1990). The sequences of new Y-linked genes were extracted based on BLAST results. We inspected all alignments of duplicates to ensure that Y-linked duplicates are distinct from the parental copies.

Cytological validation

We conducted FISH following the protocol from Larracuente and Ferree (2015). Briefly, brains from third instar larvae were dissected and collected in 1× PBS, followed by an 8-min treat of hypotonic solution (0.5% sodium citrate), fixed in 1.8% paraformaldehyde and 45% acetic acid, and dehydrated in ethanol. The 193XP probe was made by IDT with 5′-56-FAM/ACATTGGTCAAATGTCAA TATGTGGTTATGAATCC-3′ (Supplemental Table S14). Slides are mounted in Diamond Antifade Mountant with DAPI (Invitrogen) and visualized on a Leica DM5500 upright fluorescence microscope, imaged with a Hamamatsu Orca R2 CCD camera, and analyzed using Leica’s LAX software.

Data access

All raw genomic data and RNA-seq data generated in this study have been deposited to NCBI. The accession numbers of the assemblies, Illumina, and Pacific Biosciences raw reads are provided in Supplemental Table S17.

Competing interest statement

The authors declare no competing interests.

Acknowledgments

This work was funded by the National Institutes of Health (NIH) (K99GM129411 to M.C., R35GM119515 to A.M.L., R01GM123303 to J.J.E., R01GM123194 to C.D.M.) and National Science Foundation (NSF MCB 1844693 to A.M.L., NSF DDIG 1209536 to J.V., IOS-1656260 to J.J.E., NSF GRFP 1342962 to J.R.A.) and funding from the University of Nebraska-Lincoln to C.D.M. and K.L.M. and the University of California, Irvine to J.J.E. A.M.L. was supported by a Stephen Biggar and Elisabeth Asaro fellowship in Data Science. C.-H.C. was supported by the Messersmith Fellowship from the University of Rochester and the Government Scholarship to Study Abroad from Taiwan. This work was made possible, in part, through access to the Genomics High-Throughput Facility Shared Resource of the Cancer Center support grant CA-62203 at the University of California, Irvine, and NIH shared-instrumentation grants 1S10RR025496-01, 1S10OD010794-01, and 1S10OD021718-01. We also thank the University of Rochester Center for Integrated Research Computing for access to computing cluster resources. We thank Drs. Daniel Garrigan and Sarah Kingan for generating *D. sechellia* transcriptome data. We also thank Nishant Nirale, Luna Thanh Ngo, and Cécile Courret for help with data collection and management and Brandon Cooper, Christina Muirhead, Robert Kofler, Casey Bergman, and Grace Lee for comments on the manuscript.

References

- The 1000 Genomes Project Consortium. 2015. A global reference for human genetic variation. *Nature* **526**: 68–74. doi:10.1038/nature15393
- Alkan C, Sajjadian S, Eichler EE. 2011. Limitations of next-generation genome sequence assembly. *Nat Methods* **8**: 61–65. doi:10.1038/nmeth.1527
- Altschul SF, Gish W, Miller W, Myers EW, Lipman DJ. 1990. Basic local alignment search tool. *J Mol Biol* **215**: 403–410. doi:10.1016/S0022-2836(05)80360-2
- Aminetzach YT, Macpherson JM, Petrov DA. 2005. Pesticide resistance via transposition-mediated adaptive gene truncation in *Drosophila*. *Science* **309**: 764–767. doi:10.1126/science.1112699
- Arañe LO, Tao Y, Lemos B. 2016. Interspecific Y chromosome variation is sufficient to rescue hybrid male sterility and is influenced by the grandparental origin of the chromosomes. *Heredity (Edinb)* **116**: 516–522. doi:10.1038/hdy.2016.11
- Aravin AA, Hannon GJ, Brennecke J. 2007. The Piwi-piRNA pathway provides an adaptive defense in the transposon arms race. *Science* **318**: 761–764. doi:10.1126/science.1146484
- Arguello JR, Chen Y, Yang S, Wang W, Long M. 2006. Origin of an X-linked chimeric gene by illegitimate recombination in *Drosophila*. *PLoS Genet* **2**: e77. doi:10.1371/journal.pgen.0020077
- Atlan A, Mercot H, Landre C, Montchamp-Moreau C. 1997. The sex-ratio trait in *Drosophila simulans*: geographical distribution of distortion and resistance. *Evolution (N Y)* **51**: 1886–1895. doi:10.1111/j.1558-5646.1997.tb05111.x
- Bachtrog D. 2004. Evidence that positive selection drives Y-chromosome degeneration in *Drosophila miranda*. *Nat Genet* **36**: 518–522. doi:10.1038/ng1347
- Barbash DA. 2010. Ninety years of *Drosophila melanogaster* hybrids. *Genetics* **186**: 1–8. doi:10.1534/genetics.110.121459

- Bargues N, Lerat E. 2017. Evolutionary history of LTR-retrotransposons among 20 *Drosophila* species. *Mob DNA* **8**: 7. doi:10.1186/s13100-017-0090-3
- Basting PJ, Bergman CM. 2019. Complete genome assemblies for three variants of the *Wolbachia* endosymbiont of *Drosophila melanogaster*. *Microbiol Resour Annot* **8**: e00956-19. doi:10.1128/MRA.00956-19
- Battlay P, Leblanc PB, Green L, Garud NR, Schmidt JM, Fournier-Level A, Robin C. 2018. Structural variants and selective sweep foci contribute to insecticide resistance in the *Drosophila* genetic reference panel. *G3* **8**: 3489–3497. doi:10.1534/g3.118.200619
- Bayes JJ, Malik HS. 2009. Altered heterochromatin binding by a hybrid sterility protein in *Drosophila* sibling species. *Science* **326**: 1538–1541. doi:10.1126/science.1181756
- Begun DJ, Holloway AK, Stevens K, Hillier LW, Poh Y-P, Hahn MW, Nista PM, Jones CD, Kern AD, Dewey CN, et al. 2007. Population genomics: whole-genome analysis of polymorphism and divergence in *Drosophila simulans*. *PLoS Biol* **5**: e310. doi:10.1371/journal.pbio.0050310
- Bergman CM, Bensasson D. 2007. Recent LTR retrotransposon insertion contrasts with waves of non-LTR insertion since speciation in *Drosophila melanogaster*. *Proc Natl Acad Sci* **104**: 11340–11345. doi:10.1073/pnas.0702552104
- Bergman CM, Quesneville H, Anxolabéhère D, Ashburner M. 2006. Recurrent insertion and duplication generate networks of transposable element sequences in the *Drosophila melanogaster* genome. *Genome Biol* **7**: R112. doi:10.1186/gb-2006-7-11-112
- Berlin K, Koren S, Chin C-S, Drake JP, Landolin JM, Phillippy AM. 2015. Assembling large genomes with single-molecule sequencing and locality-sensitive hashing. *Nat Biotechnol* **33**: 623–630. doi:10.1038/nbt.3238
- Bhutkar A, Schaeffer SW, Russo SM, Xu M, Smith TF, Gelbart WM. 2008. Chromosomal rearrangement inferred from comparisons of 12 *Drosophila* genomes. *Genetics* **179**: 1657–1680. doi:10.1534/genetics.107.086108
- Blumenstiel JP. 2019. Birth, school, work, death, and resurrection: the life stages and dynamics of transposable element proliferation. *Genes (Basel)* **10**: 336. doi:10.3390/genes10050336
- Blumenstiel JP, Hartl DL, Lozovsky ER. 2002. Patterns of insertion and deletion in contrasting chromatin domains. *Mol Biol Evol* **19**: 2211–2225. doi:10.1093/oxfordjournals.molbev.a004045
- Bowen NJ, McDonald JF. 2001. *Drosophila* euchromatic LTR retrotransposons are much younger than the host species in which they reside. *Genome Res* **11**: 1527–1540. doi:10.1101/gr.164201
- Branco AT, Tao Y, Hartl DL, Lemos B. 2013. Natural variation of the Y chromosome suppresses sex ratio distortion and modulates testis-specific gene expression in *Drosophila simulans*. *Heredity (Edinb)* **111**: 8–15. doi:10.1038/hdy.2013.5
- Brand CL, Cattani MV, Kingan SB, Landeen EL, Presgraves DC. 2018. Molecular evolution at a meiosis gene mediates species differences in the rate and patterning of recombination. *Curr Biol* **28**: 1289–1295.e4. doi:10.1016/j.cub.2018.02.056
- Brennecke J, Aravin AA, Stark A, Dus M, Kellis M, Sachidanandam R, Hannon GJ. 2007. Discrete small RNA-generating loci as master regulators of transposon activity in *Drosophila*. *Cell* **128**: 1089–1103. doi:10.1016/j.cell.2007.01.043
- Britten RJ, Kohne DE. 1968. Repeated sequences in DNA: hundreds of thousands of copies of DNA sequences have been incorporated into the genomes of higher organisms. *Science* **161**: 529–540. doi:10.1126/science.161.3841.529
- Brown EJ, Nguyen AH, Bachtrog D. 2020. The Y chromosome may contribute to sex-specific ageing in *Drosophila*. *Nat Ecol Evol* **4**: 853–862. doi:10.1038/s41559-020-1179-5
- Cabot EL, Doshi P, Wu ML, Wu CI. 1993. Population genetics of tandem repeats in centromeric heterochromatin: unequal crossing over and chromosomal divergence at the responder locus of *Drosophila melanogaster*. *Genetics* **135**: 477–487.
- Carvalho AB, Vicoso B, Russo CAM, Swenor B, Clark AG. 2015. Birth of a new gene on the Y chromosome of *Drosophila melanogaster*. *Proc Natl Acad Sci* **112**: 12450–12455. doi:10.1073/pnas.1516543112
- Case LK, Wall EH, Osmanski EE, Dragon JA, Saligrama N, Zachary JF, Lemos B, Blankenhorn EP, Teuscher C. 2015. Copy number variation in Y chromosome multicopy genes is linked to a paternal parent-of-origin effect on CNS autoimmune disease in female offspring. *Genome Biol* **16**: 28. doi:10.1186/s13059-015-0591-7
- Cattani MV, Presgraves DC. 2009. Genetics and lineage-specific evolution of a lethal hybrid incompatibility between *Drosophila mauritiana* and its sibling species. *Genetics* **181**: 1545–1555. doi:10.1534/genetics.108.098392
- Chaisson MJ, Tesler G. 2012. Mapping single molecule sequencing reads using basic local alignment with successive refinement (BLASR): application and theory. *BMC Bioinformatics* **13**: 238. doi:10.1186/1471-2105-13-238
- Chaisson MJP, Huddleston J, Dennis MY, Sudmant PH, Malig M, Hormozdiari F, Antonacci F, Surti U, Sandstrom R, Boitano M, et al. 2015. Resolving the complexity of the human genome using single-molecule sequencing. *Nature* **517**: 608–611. doi:10.1038/nature13907
- Chaisson MJP, Sanders AD, Zhao X, Malhotra A, Porubsky D, Rausch T, Gardner EJ, Rodriguez OL, Guo L, Collins RL, et al. 2019. Multi-platform discovery of haplotype-resolved structural variation in human genomes. *Nat Commun* **10**: 1784. doi:10.1038/s41467-018-08148-z
- Chakraborty M, Fry JD. 2015. Parallel functional changes in independent testis-specific duplicates of aldehyde dehydrogenase in *Drosophila*. *Mol Biol Evol* **32**: 1029–1038. doi:10.1093/molbev/msu407
- Chakraborty M, Baldwin-Brown JG, Long AD, Emerson JJ. 2016. Contiguous and accurate de novo assembly of metazoan genomes with modest long read coverage. *Nucleic Acids Res* **44**: e147. doi:10.1093/nar/gkw654
- Chakraborty M, VanKuren NW, Zhao R, Zhang X, Kalsow S, Emerson JJ. 2018. Hidden genetic variation shapes the structure of functional elements in *Drosophila*. *Nat Genet* **50**: 20–25. doi:10.1038/s41588-017-0010-y
- Chakraborty M, Emerson JJ, Macdonald SJ, Long AD. 2019. Structural variants exhibit widespread allelic heterogeneity and shape variation in complex traits. *Nat Commun* **10**: 4872. doi:10.1038/s41467-019-12884-1
- Chakraborty M, Ramaiah A, Adolphi A, Halas P, Kaduskar B, Ngo LT, Jayaprasad S, Paul K, Whadgar S, Srinivasan S, et al. 2020. Hidden features of the malaria vector mosquito, *Anopheles stephensi*, revealed by a high-quality reference genome. bioRxiv doi:10.1101/2020.05.24.113019
- Chang C-H, Larracuent AM. 2019. Heterochromatin-enriched assemblies reveal the sequence and organization of the *Drosophila melanogaster* Y chromosome. *Genetics* **211**: 333–348. doi:10.1534/genetics.118.301765
- Chang C-H, Chavan A, Palladino J, Wei X, Martins NMC, Santinello B, Chen C-C, Erceg J, Beliveau BJ, Wu C-T, et al. 2019. Islands of retroelements are major components of *Drosophila* centromeres. *PLoS Biol* **17**: e3000241. doi:10.1371/journal.pbio.3000241
- Chin C-S, Alexander DH, Marks P, Klammer AA, Drake J, Heiner C, Clum A, Copeland A, Huddleston J, Eichler EE, et al. 2013. Nonhybrid, finished microbial genome assemblies from long-read SMRT sequencing data. *Nat Methods* **10**: 563–569. doi:10.1038/nmeth.2474
- Chippindale AK, Rice WR. 2001. Y chromosome polymorphism is a strong determinant of male fitness in *Drosophila melanogaster*. *Proc Natl Acad Sci* **98**: 5677–5682. doi:10.1073/pnas.101456898
- Chrostek E, Teixeira L. 2018. Within host selection for faster replicating bacterial symbionts. *PLoS One* **13**: e0191530. doi:10.1371/journal.pone.0191530
- Chung W-J, Okamura K, Martin R, Lai EC. 2008. Endogenous RNA interference provides a somatic defense against *Drosophila* transposons. *Curr Biol* **18**: 795–802. doi:10.1016/j.cub.2008.05.006
- Cocquet J, Ellis PJJ, Mahadevaiah SK, Affara NA, Vaiman D, Burgoyne PS. 2012. A genetic basis for a postmeiotic X versus Y chromosome intragenomic conflict in the mouse. *PLoS Genet* **8**: e1002900. doi:10.1371/journal.pgen.1002900
- Cooley L, Kelley R, Spradling A. 1988. Insertional mutagenesis of the *Drosophila* genome with single P elements. *Science* **239**: 1121–1128. doi:10.1126/science.2830671
- Cooper BS, Ginsberg PS, Turelli M, Matute DR. 2017. Wolbachia in the *Drosophila yakuba* complex: pervasive frequency variation and weak cytoplasmic incompatibility, but no apparent effect on reproductive isolation. *Genetics* **205**: 333–351. doi:10.1534/genetics.116.196238
- Coyne JA, Orr HA. 1989. Two rules of speciation. In *Speciation and its consequences* (ed. Otte D, Endler J), pp. 180–207. Sinauer, Sunderland, MA.
- Cridland JM, Macdonald SJ, Long AD, Thornton KR. 2013. Abundance and distribution of transposable elements in Two *Drosophila* QTL mapping resources. *Mol Biol Evol* **30**: 2311–2327. doi:10.1093/molbev/mst129
- Daborn PJ, Yen JL, Bogwitz MR, Le Goff G, Feil E, Jeffers S, Tijet N, Perry T, Heckel D, Batterham P, et al. 2002. A single p450 allele associated with insecticide resistance in *Drosophila*. *Science* **297**: 2253–2256. doi:10.1126/science.1074170
- Darling AE, Mau B, Perna NT. 2010. ProgressiveMauve: multiple genome alignment with gene gain, loss and rearrangement. *PLoS One* **5**: e11147. doi:10.1371/journal.pone.0011147
- Delabaere L, Orsi GA, Sapey-Triomphe L, Horard B, Couble P, Loppin B. 2014. The spartan ortholog maternal haploid is required for paternal chromosome integrity in the *Drosophila* zygote. *Curr Biol* **24**: 2281–2287. doi:10.1016/j.cub.2014.08.010
- DiBartolomeis SM, Tartof KD, Jackson FR. 1992. A superfamily of *Drosophila* satellite related (SR) DNA repeats restricted to the X chromosome euchromatin. *Nucleic Acids Res* **20**: 1113–1116. doi:10.1093/nar/20.5.1113
- Ding Y, Zhao L, Yang S, Jiang Y, Chen Y, Zhao R, Zhang Y, Zhang G, Dong Y, Yu H, et al. 2010. A young *Drosophila* duplicate gene plays essential roles

- in spermatogenesis by regulating several Y-linked male fertility genes. *PLoS Genet* **6**: e1001255. doi:10.1371/journal.pgen.1001255
- Ding Y, Lillvis JL, Cande J, Berman GJ, Arthur BJ, Long X, Xu M, Dickson BJ, Stern DL. 2019. Neural evolution of context-dependent fly song. *Curr Biol* **29**: 1089–1099.e7. doi:10.1016/j.cub.2019.02.019
- Doolittle WF, Sapienza C. 1980. Selfish genes, the phenotype paradigm and genome evolution. *Nature* **284**: 601–603. doi:10.1038/284601a0
- Dowsett AP, Young MW. 1982. Differing levels of dispersed repetitive DNA among closely related species of *Drosophila*. *Proc Natl Acad Sci* **79**: 4570–4574. doi:10.1073/pnas.79.15.4570
- Drosophila* 12 Genomes Consortium. 2007. Evolution of genes and genomes on the *Drosophila* phylogeny. *Nature* **450**: 203–218. doi:10.1038/nature06341
- Edgar RC. 2004. MUSCLE: multiple sequence alignment with high accuracy and high throughput. *Nucleic Acids Res* **32**: 1792–1797. doi:10.1093/nar/gkh340
- Eickbush MT, Young JM, Zanders SE. 2019. Killer meiotic drive and dynamic evolution of the wtf gene family. *Mol Biol Evol* **36**: 1201–1214. doi:10.1093/molbev/msz052
- Ellis PJI, Bacon J, Affara NA. 2011. Association of Sly with sex-linked gene amplification during mouse evolution: a side effect of genomic conflict in spermatids? *Hum Mol Genet* **20**: 3010–3021. doi:10.1093/hmg/ddr204
- Ellison CE, Bachtrog D. 2013. Dosage compensation via transposable element mediated rewiring of a regulatory network. *Science* **342**: 846–850. doi:10.1126/science.1239552
- Ellison C, Bachtrog D. 2019. Recurrent gene co-amplification on *Drosophila* X and Y chromosomes. *PLoS Genet* **15**: e1008251. doi:10.1371/journal.pgen.1008251
- Faddeeva-Vakhrusheva A, Kraaijeveld K, Derks MFL, Anvar SY, Agamennone V, Suring W, Kampfraath AA, Ellers J, Le Ngoc G, van Gestel CAM, et al. 2017. Coping with living in the soil: the genome of the parthenogenetic springtail *Folsomia candida*. *BMC Genomics* **18**: 493. doi:10.1186/s12864-017-3852-x
- Ferree PM, Barbash DA. 2009. Species-specific heterochromatin prevents mitotic chromosome segregation to cause hybrid lethality in *Drosophila*. *PLoS Biol* **7**: e1000234. doi:10.1371/journal.pbio.1000234
- Feschotte C. 2008. Transposable elements and the evolution of regulatory networks. *Nat Rev Genet* **9**: 397–405. doi:10.1038/nrg2337
- Fishman L, Saunders A. 2008. Centromere-associated female meiotic drive entails male fitness costs in monkeyflowers. *Science* **322**: 1559–1562. doi:10.1126/science.1161406
- Flutur T, Duprat E, Feuillet C, Quesneville H. 2011. Considering transposable element diversification in de novo annotation approaches. *PLoS One* **6**: e16526. doi:10.1371/journal.pone.0016526
- Gallach M. 2014. Recurrent turnover of chromosome-specific satellites in *Drosophila*. *Genome Biol Evol* **6**: 1279–1286. doi:10.1093/gbe/evu104
- Garrigan D, Kingan SB, Geneva AJ, Andolfatto P, Clark AG, Thornton KR, Presgraves DC. 2012. Genome sequencing reveals complex speciation in the *Drosophila simulans* clade. *Genome Res* **22**: 1499–1511. doi:10.1101/gr.130922.111
- Garrigan D, Kingan SB, Geneva AJ, Vedanayagam JP, Presgraves DC. 2014. Genome diversity and divergence in *Drosophila mauritiana*: multiple signatures of faster X evolution. *Genome Biol Evol* **6**: 2444–2458. doi:10.1093/gbe/evu198
- Gel B, Serra E. 2017. Karyoploter: an R/Bioconductor package to plot customizable genomes displaying arbitrary data. *Bioinformatics* **33**: 3088–3090. doi:10.1093/bioinformatics/btx346
- Gemayel R, Vences MD, Legendre M, Verstrepen KJ. 2010. Variable tandem repeats accelerate evolution of coding and regulatory sequences. *Annu Rev Genet* **44**: 445–477. doi:10.1146/annurev-genet-072610-155046
- Gordon SP, Tseng E, Salamov A, Zhang J, Meng X, Zhao Z, Kang D, Underwood J, Grigoriev IV, Figueroa M, et al. 2015. Widespread polycistronic transcripts in fungi revealed by single-molecule mRNA sequencing. *PLoS One* **10**: e0132628. doi:10.1371/journal.pone.0132628
- Harris RS. 2007. “Improved pairwise alignment of genomic DNA.” PhD thesis, The Pennsylvania State University.
- Hartley G, O’Neill RJ. 2019. Centromere repeats: hidden gems of the genome. *Genes (Basel)* **10**: 223. doi:10.3390/genes10030223
- Helleu Q, Gérard PR, Dubruielle R, Ogereau D, Prud’homme B, Loppin B, Montchamp-Moreau C. 2016. Rapid evolution of a Y-chromosome heterochromatin protein underlies sex chromosome meiotic drive. *Proc Natl Acad Sci* **113**: 4110–4115. doi:10.1073/pnas.1519332113
- Henikoff S, Ahmad K, Malik HS. 2001. The centromere paradox: stable inheritance with rapidly evolving DNA. *Science* **293**: 1098–1102. doi:10.1126/science.1062939
- Hey J, Kliman RM. 1993. Population genetics and phylogenetics of DNA sequence variation at multiple loci within the *Drosophila melanogaster* species complex. *Mol Biol Evol* **10**: 804–822. doi:10.1093/oxfordjournals.molbev.a040044
- Hoffman AA, Turelli M. 1997. Cytoplasmic incompatibility in insects. In *Influential passengers* (ed. O’Neill SL, et al.), pp. 42–80. Oxford University Press, New York.
- Holt C, Yandell M. 2011. MAKER2: an annotation pipeline and genome-database management tool for second-generation genome projects. *BMC Bioinformatics* **12**: 491. doi:10.1186/1471-2105-12-491
- Hoskins RA, Smith CD, Carlson JW, Carvalho AB, Halpern A, Kaminker JS, Kennedy C, Mungall CJ, Sullivan BA, Sutton GG, et al. 2002. Heterochromatic sequences in a *Drosophila* whole-genome shotgun assembly. *Genome Biol* **3**: RESEARCH0085. doi:10.1186/gb-2002-3-12-research0085
- Hoskins RA, Carlson JW, Wan KH, Park S, Mendez I, Galle SE, Booth BW, Pfeiffer BD, George RA, Svirskas R, et al. 2015. The release 6 reference sequence of the *Drosophila melanogaster* genome. *Genome Res* **25**: 445–458. doi:10.1101/gr.185579.114
- Hu TT, Eisen MB, Thornton KR, Andolfatto P. 2013. A second-generation assembly of the *Drosophila simulans* genome provides new insights into patterns of lineage-specific divergence. *Genome Res* **23**: 89–98. doi:10.1101/gr.141689.112
- International Human Genome Sequencing Consortium. 2001. Initial sequencing and analysis of the human genome. *Nature* **409**: 860–921. doi:10.1038/35057062
- Jaenike J. 2001. Sex chromosome meiotic drive. *Annu Rev Ecol Syst* **32**: 25–49. doi:10.1146/annurev.ecolsys.32.081501.113958
- Jagannathan M, Warsinger-Pepe N, Watase GJ, Yamashita YM. 2017. Comparative analysis of satellite DNA in the *Drosophila melanogaster* species complex. *G3* **7**: 693–704. doi:10.1534/g3.116.035352
- Kaminker JS, Bergman CM, Kronmiller B, Carlson J, Svirskas R, Patel S, Frise E, Wheeler DA, Lewis SE, Rubin GM, et al. 2002. The transposable elements of the *Drosophila melanogaster* euchromatin: a genomics perspective. *Genome Biol* **3**: research0084.1. doi:10.1186/gb-2002-3-12-research0084
- Kampfraath AA, Klasson L, Anvar SY, Vossen RHAM, Roelofs D, Kraaijeveld K, Ellers J. 2019. Genome expansion of an obligate parthenogenesis-associated *Wolbachia* poses an exception to the symbiont reduction model. *BMC Genomics* **20**: 106. doi:10.1186/s12864-019-5492-9
- Katju V, Lynch M. 2006. On the formation of novel genes by duplication in the *Caenorhabditis elegans* genome. *Mol Biol Evol* **23**: 1056–1067. doi:10.1093/molbev/msj114
- Keightley PD, Ness RW, Halligan DL, Haddrill PR. 2014. Estimation of the spontaneous mutation rate per nucleotide site in a *Drosophila melanogaster* full-sib family. *Genetics* **196**: 313–320. doi:10.1534/genetics.113.158758
- Kelleher ES, Jaweria J, Akoma U, Ortega L, Tang W. 2018. QTL mapping of natural variation reveals that the developmental regulator *bruno* reduces tolerance to P-element transposition in the *Drosophila* female germline. *PLoS Biol* **16**: e2006040. doi:10.1371/journal.pbio.2006040
- Kent WJ, Baertsch R, Hinrichs A, Miller W, Haussler D. 2003. Evolution’s cauldron: duplication, deletion, and rearrangement in the mouse and human genomes. *Proc Natl Acad Sci* **100**: 11484–11489. doi:10.1073/pnas.1932072100
- Khost DE, Eickbush DG, Larracuente AM. 2017. Single-molecule sequencing resolves the detailed structure of complex satellite DNA loci in *Drosophila melanogaster*. *Genome Res* **27**: 709–721. doi:10.1101/gr.213512.116
- Klein SJ, O’Neill RJ. 2018. Transposable elements: genome innovation, chromosome diversity, and centromere conflict. *Chromosome Res* **26**: 5–23. doi:10.1007/s10577-017-9569-5
- Kliman RM, Andolfatto P, Coyne JA, Depaulis F, Kreitman M, Berry AJ, McCarter J, Wakeley J, Hey J. 2000. The population genetics of the origin and divergence of the *Drosophila simulans* complex species. *Genetics* **156**: 1913–1931.
- Koerich LB, Wang X, Clark AG, Carvalho AB. 2008. Low conservation of gene content in the *Drosophila* Y chromosome. *Nature* **456**: 949–951. doi:10.1038/nature07463
- Kofler R, Betancourt AJ, Schlötterer C. 2012. Sequencing of pooled DNA samples (Pool-Seq) uncovers complex dynamics of transposable element insertions in *Drosophila melanogaster*. *PLoS Genet* **8**: e1002487. doi:10.1371/journal.pgen.1002487
- Kofler R, Nolte V, Schlötterer C. 2015. Tempo and mode of transposable element activity in *Drosophila*. *PLoS Genet* **11**: e1005406. doi:10.1371/journal.pgen.1005406
- Kopp A, Frank AK, Barmina O. 2006. Interspecific divergence, intrachromosomal recombination, and phylogenetic utility of Y-chromosomal genes in *Drosophila*. *Mol Phylogenet Evol* **38**: 731–741. doi:10.1016/j.ympev.2005.10.006
- Koren S, Walenz BP, Berlin K, Miller JR, Bergman NH, Phillippy AM. 2017. Canu: scalable and accurate long-read assembly via adaptive k-mer weighting and repeat separation. *Genome Res* **27**: 722–736. doi:10.1101/gr.215087.116

- Koren S, Rhie A, Walenz BP, Dilthey AT, Bickhart DM, Kingan SB, Hiendleder S, Williams JL, Smith TPL, Phillippy AM. 2018. De novo assembly of haplotype-resolved genomes with trio binning. *Nat Biotechnol* **36**: 1174–1182. doi:10.1038/nbt.4277
- Kriesner P, Hoffmann AA, Lee SF, Turelli M, Weeks AR. 2013. Rapid sequential spread of two *Wolbachia* variants in *Drosophila simulans*. *PLoS Pathog* **9**: e1003607. doi:10.1371/journal.ppat.1003607
- Kriesner P, Conner WR, Weeks AR, Turelli M, Hoffmann AA. 2016. Persistence of a *Wolbachia* infection frequency cline in *Drosophila melanogaster* and the possible role of reproductive dormancy. *Evolution* **70**: 979–997. doi:10.1111/evo.12923
- Krsticevic FJ, Schrago CG, Carvalho AB. 2015. Long-read single molecule sequencing to resolve tandem gene copies: the Mst77Y region on the *Drosophila melanogaster* Y chromosome. *G3* **5**: 1145–1150. doi:10.1534/g3.115.017277
- Kruger AN, Brogley MA, Huizinga JL, Kidd JM, de Rooij DG, Hu Y-C, Mueller JL. 2019. A neofunctionalized X-linked ampliconic gene family is essential for male fertility and equal sex ratio in mice. *Curr Biol* **29**: 3699–3706.e5. doi:10.1016/j.cub.2019.08.057
- Kuhn GC, Küttler H, Moreira-Filho O, Heslop-Harrison JS. 2012. The 1.688 repetitive DNA of *Drosophila*: concerted evolution at different genomic scales and association with genes. *Mol Biol Evol* **29**: 7–11. doi:10.1093/molbev/msr173
- Kutch IC, Fedorka KM. 2015. Y-linked variation for autosomal immune gene regulation has the potential to shape sexually dimorphic immunity. *Proc Biol Sci* **282**: 20151301. doi:10.1098/rspb.2015.1301
- Laetsch DR, Blaxter ML. 2017. Blobtools: interrogation of genome assemblies. *F1000Res* **6**: 1287. doi:10.12688/f1000research.12232.1
- Larracuente AM. 2014. The organization and evolution of the *Responder* satellite in species of the *Drosophila melanogaster* group: dynamic evolution of a target of meiotic drive. *BMC Evol Biol* **14**: 233. doi:10.1186/s12862-014-0233-9
- Larracuente AM, Clark AG. 2013. Surprising differences in the variability of Y chromosomes in African and cosmopolitan populations of *Drosophila melanogaster*. *Genetics* **193**: 201–214. doi:10.1534/genetics.112.146167
- Larracuente AM, Ferree PM. 2015. Simple method for fluorescence DNA *in situ* hybridization to squashed chromosomes. *J Vis Exp* **95**: 52288. doi:10.3791/52288
- Larracuente AM, Presgraves DC. 2012. The selfish *Segregation Distorter* gene complex of *Drosophila melanogaster*. *Genetics* **192**: 33–53. doi:10.1534/genetics.112.141390
- Lee YCG, Karpen GH. 2017. Pervasive epigenetic effects of *Drosophila* eukaryotic transposable elements impact their evolution. *eLife* **6**: e25762. doi:10.7554/eLife.25762
- Lefoulon E, Vaisman N, Frydman HM, Sun L, Voland L, Foster JM, Slatko BE. 2019. Large enriched fragment targeted sequencing (LEFT-SEQ) applied to capture of *Wolbachia* genomes. *Sci Rep* **9**: 5939. doi:10.1038/s41598-019-42454-w
- Lemos B, Branco AT, Hartl DL. 2010. Epigenetic effects of polymorphic Y chromosomes modulate chromatin components, immune response, and sexual conflict. *Proc Natl Acad Sci* **107**: 15826–15831. doi:10.1073/pnas.1010383107
- Lerat E, Bulet N, Biémont C, Vieira C. 2011. Comparative analysis of transposable elements in the melanogaster subgroup sequenced genomes. *Gene* **473**: 100–109. doi:10.1016/j.gene.2010.11.009
- Li H. 2016. Minimap and miniasm: fast mapping and de novo assembly for noisy long sequences. *Bioinformatics* **32**: 2103–2110. doi:10.1093/bioinformatics/btw152
- Li H. 2018. Minimap2: pairwise alignment for nucleotide sequences. *Bioinformatics* **34**: 3094–3100. doi:10.1093/bioinformatics/bty191
- Lin Y, Moret BME. 2008. Estimating true evolutionary distances under the DCJ model. *Bioinformatics* **24**: i114–i122. doi:10.1093/bioinformatics/btn148
- Lindholm AK, Dyer KA, Firman RC, Fishman L, Forstmeier W, Holman L, Johannesson H, Knief U, Kokko H, Larracuente AM, et al. 2016. The ecology and evolutionary dynamics of meiotic drive. *Trends Ecol Evol* **31**: 315–326. doi:10.1016/j.tree.2016.02.001
- Lipatov M, Lenkov K, Petrov DA, Bergman CM. 2005. Paucity of chimeric gene-transposable element transcripts in the *Drosophila melanogaster* genome. *BMC Biol* **3**: 24. doi:10.1186/1741-7007-3-24
- Lohe AR, Brutlag DL. 1987. Identical satellite DNA sequences in sibling species of *Drosophila*. *J Mol Biol* **194**: 161–170. doi:10.1016/0022-2836(87)90365-2
- Lohe AR, Roberts PA. 1990. An unusual Y chromosome of *Drosophila simulans* carrying amplified rDNA spacer without rRNA genes. *Genetics* **125**: 399–406.
- Long M, Betrán E, Thornton K, Wang W. 2003. The origin of new genes: glimpses from the young and old. *Nat Rev Genet* **4**: 865–875. doi:10.1038/nrg1204
- Loppin B, Berger F, Couble P. 2001. Paternal chromosome incorporation into the zygote nucleus is controlled by maternal haploid in *Drosophila*. *Dev Biol* **231**: 383–396. doi:10.1006/dbio.2000.0152
- Lowe TM, Eddy SR. 1997. tRNAscan-SE: a program for improved detection of transfer RNA genes in genomic sequence. *Nucleic Acids Res* **25**: 955–964. doi:10.1093/nar/25.5.955
- Lower SS, McGurk MP, Clark AG, Barbash DA. 2018. Satellite DNA evolution: old ideas, new approaches. *Curr Opin Genet Dev* **49**: 70–78. doi:10.1016/j.cde.2018.03.003
- Lynch M, Force AG. 2000. The origin of interspecific genomic incompatibility via gene duplication. *Am Nat* **156**: 590–605. doi:10.1086/316992
- Mahajan S, Wei KH-C, Nalley MJ, Gibilisco L, Bachtrög D. 2018. De novo assembly of a young *Drosophila* Y chromosome using single-molecule sequencing and chromatin conformation capture. *PLoS Biol* **16**: e2006348. doi:10.1371/journal.pbio.2006348
- Manee MM, Jackson J, Bergman CM. 2018. Conserved noncoding elements influence the transposable element landscape in *Drosophila*. *Genome Biol Evol* **10**: 1533–1545. doi:10.1093/gbe/evy104
- Marçais G, Delcher AL, Phillippy AM, Coston R, Salzberg SL, Zimin A. 2018. MUMmer4: a fast and versatile genome alignment system. *PLoS Comput Biol* **14**: e1005944. doi:10.1371/journal.pcbi.1005944
- Masly JP, Presgraves DC. 2007. High-resolution genome-wide dissection of the two roles of speciation in *Drosophila*. *PLoS Biol* **5**: e243. doi:10.1371/journal.pbio.0050243
- Mason JM, Frydrychova RC, Biessmann H. 2008. *Drosophila* telomeres: an exception providing new insights. *Bioessays* **30**: 25–37. doi:10.1002/bies.20688
- Mazo AM, Mizrokhi LJ, Karavanov AA, Sedkov YA, Krichevskaja AA, Ilyin YV. 1989. Suppression in *Drosophila*: su(Hw) and su(f) gene products interact with a region of gypsy (mdg4) regulating its transcriptional activity. *EMBO J* **8**: 903–911. doi:10.1002/j.1460-2075.1989.tb03451.x
- McBride CS. 2007. Rapid evolution of smell and taste receptor genes during host specialization in *Drosophila sechellia*. *Proc Natl Acad Sci* **104**: 4996–5001. doi:10.1073/pnas.0608424104
- Meany MK, Conner WR, Richter SV, Bailey JA, Turelli M, Cooper BS. 2019. Loss of cytoplasmic incompatibility and minimal fecundity effects explain relatively low *Wolbachia* frequencies in *Drosophila mauritiana*. *Evolution (N Y)* **73**: 1278–1295. doi:10.1111/evo.13745
- Meiklejohn CD, Landeen EL, Gordon KE, Rzatkiewicz T, Kingan SB, Geneva AJ, Vedanayagam JP, Muirhead CA, Garrigan D, Stern DL, et al. 2018. Gene flow mediates the role of sex chromosome meiotic drive during complex speciation. *eLife* **7**: e35468. doi:10.7554/eLife.35468
- Menon DU, Meller VH. 2012. A role for siRNA in X-chromosome dosage compensation in *Drosophila melanogaster*. *Genetics* **191**: 1023–1028. doi:10.1534/genetics.112.140236
- Menon DU, Coarfa C, Xiao W, Gunaratne PH, Meller VH. 2014. siRNAs from an X-linked satellite repeat promote X-chromosome recognition in *Drosophila melanogaster*. *Proc Natl Acad Sci* **111**: 16460–16465. doi:10.1073/pnas.1410534111
- Merçot H, Defaye D, Capy P, Pla E, David JR. 1994. Alcohol tolerance, ADH activity, and ecological niche of *Drosophila* species. *Evolution (N Y)* **48**: 746–757. doi:10.1111/j.1558-5646.1994.tb01358.x
- Miga KH, Koren S, Rhie A, Vollger MR, Gershman A, Bzikadze A, Brooks S, Howe E, Porubsky D, Logsdon GA, et al. 2020. Telomere-to-telomere assembly of a complete human X chromosome. *Nature* **585**: 79–84. doi:10.1038/s41586-020-2547-7
- Mikheenko A, Prjibelski A, Saveliev V, Antipov D, Gurevich A. 2018. Versatile genome assembly evaluation with QUAST-LG. *Bioinformatics* **34**: i142–i150. doi:10.1093/bioinformatics/bty266
- Miller DE, Staber C, Zeitlinger J, Hawley RS. 2018. Genome report: highly contiguous genome assemblies of 15 *Drosophila* species generated using nanopore sequencing. *G3* **8**: 3131–3141. doi:10.1534/g3.118.200160
- Miyashita N, Langley CH. 1988. Molecular and phenotypic variation of the white locus region in *Drosophila melanogaster*. *Genetics* **120**: 199–212.
- Montchamp-Moreau C, Ogereau D, Chaminade N, Colard A, Aulard S. 2006. Organization of the sex-ratio meiotic drive region in *Drosophila simulans*. *Genetics* **174**: 1365–1371. doi:10.1534/genetics.105.051755
- Montgomery E, Charlesworth B, Langley CH. 1987. A test for the role of natural selection in the stabilization of transposable element copy number in a population of *Drosophila melanogaster*. *Genet Res* **49**: 31–41. doi:10.1017/S0016672300026707
- Moriyama EN, Powell JR. 1997. Codon usage bias and tRNA abundance in *Drosophila*. *J Mol Evol* **45**: 514–523. doi:10.1007/PL00006256
- Moyzis RK, Buckingham JM, Cram LS, Dani M, Deaven LL, Jones MD, Meyne J, Ratliff RL, Wu J-R. 1988. A highly conserved repetitive DNA sequence, (TTAGGG)_n, present at the telomeres of human chromosomes. *Proc Natl Acad Sci* **85**: 6622–6626. doi:10.1073/pnas.85.18.6622
- Nouhaud P. 2018. Long-read based assembly and annotation of a *Drosophila simulans* genome. bioRxiv doi:10.1101/425710

- Nuzhdin SV. 1995. The distribution of transposable elements on X chromosomes from a natural population of *Drosophila simulans*. *Genet Res* **66**: 159–166. doi:10.1017/S0016672300034509
- Orgel LE, Crick FH. 1980. Selfish DNA: the ultimate parasite. *Nature* **284**: 604–607. doi:10.1038/284604a0
- Osada N, Innan H. 2008. Duplication and gene conversion in the *Drosophila melanogaster* genome. *PLoS Genet* **4**: e1000305. doi:10.1371/journal.pgen.1000305
- Parhad SS, Theurkauf WE. 2019. Rapid evolution and conserved function of the piRNA pathway. *Open Biol* **9**: 180181. doi:10.1098/rsob.180181
- Parkhurst SM, Corces VG. 1986. Mutations at the suppressor of forked locus increase the accumulation of gypsy-encoded transcripts in *Drosophila melanogaster*. *Mol Cell Biol* **6**: 2271–2274. doi:10.1128/MCB.6.6.2271
- Pease JB, Hahn MW. 2013. More accurate phylogenies inferred from low-recombination regions in the presence of incomplete lineage sorting. *Evolution (N Y)* **67**: 2376–2384. doi:10.1111/evo.12118
- Perteu M, Kim D, Perteu GM, Leek JT, Salzberg SL. 2016. Transcript-level expression analysis of RNA-seq experiments with HISAT, stringTie and ballgown. *Nat Protoc* **11**: 1650–1667. doi:10.1038/nprot.2016.095
- Petrov DA, Hartl DL. 1998. High rate of DNA loss in the *Drosophila melanogaster* and *Drosophila virilis* species groups. *Mol Biol Evol* **15**: 293–302. doi:10.1093/oxfordjournals.molbev.a025926
- Petrov DA, Lozovskaya ER, Hartl DL. 1996. High intrinsic rate of DNA loss in *Drosophila*. *Nature* **384**: 346–349. doi:10.1038/384346a0
- Petrov DA, Fiston-Lavier A-S, Lipatov M, Lenkov K, González J. 2011. Population genomics of transposable elements in *Drosophila melanogaster*. *Mol Biol Evol* **28**: 1633–1644. doi:10.1093/molbev/msq337
- Plohl M, Meštrović N, Mravinac B. 2012. Satellite DNA evolution. *Genome Dyn* **7**: 126–152. doi:10.1159/000337122
- Presgraves DC. 2006. Intron length evolution in *Drosophila*. *Mol Biol Evol* **23**: 2203–2213. doi:10.1093/molbev/msl094
- Quesneville H, Bergman CM, Andrieu O, Autard D, Nouaud D, Ashburner M, Anxolabehere D. 2005. Combined evidence annotation of transposable elements in genome sequences. *PLoS Comput Biol* **1**: 166–175. doi:10.1371/journal.pcbi.0010022
- Quinlan AR, Hall IM. 2010. BEDTools: a flexible suite of utilities for comparing genomic features. *Bioinformatics* **26**: 841–842. doi:10.1093/bioinformatics/btq033
- Ranz JM, Maurin D, Chan YS, von Grothuss M, Hillier LW, Roote J, Ashburner M, Bergman CM. 2007. Principles of genome evolution in the *Drosophila melanogaster* species group. *PLoS Biol* **5**: e152. doi:10.1371/journal.pbio.0050152
- Rathje CC, Johnson EEP, Drage D, Patinioti C, Silvestri G, Affara NA, Ialy-Radio C, Cocquet J, Skinner BM, Ellis PJJ. 2019. Differential sperm motility mediates the sex ratio drive shaping mouse sex chromosome evolution. *Curr Biol* **29**: 3692–3698.e4. doi:10.1016/j.cub.2019.09.031
- R’Kha S, Cappy P, David JR. 1991. Host-plant specialization in the *Drosophila melanogaster* species complex: a physiological, behavioral, and genetical analysis. *Proc Natl Acad Sci* **88**: 1835–1839. doi:10.1073/pnas.88.5.1835
- Rockman MV, Wray GA. 2002. Abundant raw material for cis-regulatory evolution in humans. *Mol Biol Evol* **19**: 1991–2004. doi:10.1093/oxfordjournals.molbev.a004023
- Rogers HH, Griffiths-Jones S. 2014. tRNA anticodon shifts in eukaryotic genomes. *RNA* **20**: 269–281. doi:10.1026/rna.041681.113
- Rogers HH, Bergman CM, Griffiths-Jones S. 2010. The evolution of tRNA genes in *Drosophila*. *Genome Biol Evol* **2**: 467–477. doi:10.1093/gbe/evq034
- Rogers RL, Cridland JM, Shao L, Hu TT, Andolfatto P, Thornton KR. 2014. Landscape of standing variation for tandem duplications in *Drosophila yakuba* and *Drosophila simulans*. *Mol Biol Evol* **31**: 1750–1766. doi:10.1093/molbev/msu124
- Rotherfluh A, Threlkeld RJ, Bainton RJ, Tsai LT-Y, Lasek AW, Heberlein U. 2006. Distinct behavioral responses to ethanol are regulated by alternate RhoGAP18B isoforms. *Cell* **127**: 199–211. doi:10.1016/j.cell.2006.09.010
- Sackton TB, Kulathinal RJ, Bergman CM, Quinlan AR, Dopman EB, Carneiro M, Marth GT, Hartl DL, Clark AG. 2009. Population genomic inferences from sparse high-throughput sequencing of two populations of *Drosophila melanogaster*. *Genome Biol Evol* **1**: 449–465. doi:10.1093/gbe/evp048
- Salzberg SL, Yorke JA. 2005. Beware of mis-assembled genomes. *Bioinformatics* **21**: 4320–4321. doi:10.1093/bioinformatics/bti769
- Schaeffer SW, Bhutkar A, McAllister BF, Matsuda M, Matzkin LM, O’Grady PM, Rohde C, Valente VLS, Aguadé M, Anderson WW, et al. 2008. Polytenic chromosomal maps of 11 *Drosophila* species: the order of genomic scaffolds inferred from genetic and physical maps. *Genetics* **179**: 1601–1655. doi:10.1534/genetics.107.086074
- Schwartz S, Kent WJ, Smit A, Zhang Z, Baertsch R, Hardison RC, Haussler D, Miller W. 2003. Human–mouse alignments with BLASTZ. *Genome Res* **13**: 103–107. doi:10.1101/gr.809403
- Serbus LR, Sullivan W. 2007. A cellular basis for *Wolbachia* recruitment to the host germline. *PLoS Pathog* **3**: e190. doi:10.1371/journal.ppat.0030190
- Simão FA, Waterhouse RM, Ioannidis P, Kriventseva EV, Zdobnov EM. 2015. BUSCO: assessing genome assembly and annotation completeness with single-copy orthologs. *Bioinformatics* **31**: 3210–3212. doi:10.1093/bioinformatics/btv351
- Singh ND, Bauer DuMont VL, Hubisz MJ, Nielsen R, Aquadro CF. 2007. Patterns of mutation and selection at synonymous sites in *Drosophila*. *Mol Biol Evol* **24**: 2687–2697. doi:10.1093/molbev/msm196
- Smit AFA, Hubley R, Green P. 2013. RepeatMasker Open-4.0. <http://www.repeatmasker.org>.
- Solares EA, Chakraborty M, Miller DE, Kalsow S, Hall K, Perera AG, Emerson JJ, Hawley RS. 2018. Rapid low-cost assembly of the *Drosophila melanogaster* reference genome using Low-coverage, long-read sequencing. *G3* **8**: 3143–3154. doi:10.1534/g3.118.200162
- Sprout JS, Khost DE, Eickbush DG, Negm S, Wei X, Wong I, Larracunte AM. 2020. Dynamic evolution of euchromatic satellites on the X chromosome in *Drosophila melanogaster* and the simulans clade. *Mol Biol Evol* **37**: 2241–2256. doi:10.1093/molbev/msaa078
- Stage DE, Eickbush TH. 2007. Sequence variation within the rRNA gene loci of 12 *Drosophila* species. *Genome Res* **17**: 1888–1897. doi:10.1101/gr.6376807
- Stein JC, Yu Y, Copetti D, Zwickl DJ, Zhang L, Zhang C, Chougule K, Gao D, Iwata A, Goicoechea JL, et al. 2018. Genomes of 13 domesticated and wild rice relatives highlight genetic conservation, turnover and innovation across the genus *Oryza*. *Nat Genet* **50**: 285–296. doi:10.1038/s41588-018-0040-0
- Steinberg KM, Schneider VA, Graves-Lindsay TA, Fulton RS, Agarwala R, Huddleston J, Shiryev SA, Morgulis A, Surti U, Warren WC, et al. 2014. Single haplotype assembly of the human genome from a hydatidiform mole. *Genome Res* **24**: 2066–2076. doi:10.1101/gr.180893.114
- Stitzer MC, Anderson SN, Springer NM, Ross-Ibarra J. 2019. The genomic ecosystem of transposable elements in maize. bioRxiv doi:10.1101/559922
- Sturtevant AH, Plunkett CR. 1926. Sequence of corresponding third-chromosome genes in *Drosophila melanogaster* and *D. simulans*. *Biol Bull* **50**: 56–60. doi:10.2307/1536631
- Talbert P, Kasinathan S, Henikoff S. 2018. Simple and complex centromeric satellites in *Drosophila* sibling species. *Genetics* **208**: 977–990. doi:10.1534/genetics.117.300620
- Tang X, Cao J, Zhang L, Huang Y, Zhang Q, Rong YS. 2017. Maternal haploid, a metalloprotease enriched at the largest satellite repeat and essential for genome integrity in *Drosophila* embryos. *Genetics* **206**: 1829–1839. doi:10.1534/genetics.117.200949
- Tao Y, Hartl DL. 2003. Genetic dissection of hybrid incompatibilities between *Drosophila simulans* and *D. mauritiana*. III. Heterogeneous accumulation of hybrid incompatibilities, degree of dominance, and implications for Haldane’s rule. *Evolution (N Y)* **57**: 2580–2598. doi:10.1111/j.0014-3820.2003.tb01501.x
- Tao Y, Hartl DL, Laurie CC. 2001. Sex-ratio segregation distortion associated with reproductive isolation in *Drosophila*. *Proc Natl Acad Sci* **98**: 13183–13188. doi:10.1073/pnas.231478798
- Tao Y, Araripe L, Kingan SB, Ke Y, Xiao H, Hartl DL. 2007a. A sex-ratio meiotic drive system in *Drosophila simulans*. II: an X-linked distorter. *PLoS Biol* **5**: e293. doi:10.1371/journal.pbio.0050293
- Tao Y, Masly JP, Araripe L, Ke Y, Hartl DL. 2007b. A sex-ratio meiotic drive system in *Drosophila simulans*. I: an autosomal suppressor. *PLoS Biol* **5**: e292. doi:10.1371/journal.pbio.0050292
- Ting C-T, Tsaur S-C, Sun S, Browne WE, Chen Y-C, Patel NH, Wu C-I. 2004. Gene duplication and speciation in *Drosophila*: evidence from the Odysseus locus. *Proc Natl Acad Sci* **101**: 12232–12235. doi:10.1073/pnas.0401975101
- Tobler R, Nolte V, Schlötterer C. 2017. High rate of translocation-based gene birth on the *Drosophila* Y chromosome. *Proc Natl Acad Sci* **114**: 11721–11726. doi:10.1073/pnas.1706502114
- Treangen TJ, Salzberg SL. 2012. Repetitive DNA and next-generation sequencing: computational challenges and solutions. *Nat Rev Genet* **13**: 36–46. doi:10.1038/nrg3117
- True JR, Mercer JM, Laurie CC. 1996. Differences in crossover frequency and distribution among three sibling species of *Drosophila*. *Genetics* **142**: 507–523.
- Turelli M, Hoffmann AA. 1995. Cytoplasmic incompatibility in *Drosophila simulans*: dynamics and parameter estimates from natural populations. *Genetics* **140**: 1319–1338.
- Unckless RL, Larracunte AM, Clark AG. 2015. Sex-ratio meiotic drive and Y-linked resistance in *Drosophila affinis*. *Genetics* **199**: 831–840. doi:10.1534/genetics.114.173948
- Van’t Hof AE, Campagne P, Rigden DJ, Yung CJ, Lingley J, Quail MA, Hall N, Darby AC, Saccheri IJ. 2016. The industrial melanism mutation in

- British peppered moths is a transposable element. *Nature* **534**: 102–105. doi:10.1038/nature17951
- Velandia-Huerto CA, Berkemer SJ, Hoffmann A, Retzlaff N, Romero Marroquín LC, Hernández-Rosales M, Stadler PF, Bermúdez-Santana CI. 2016. Orthologs, turn-over, and remodeling of tRNAs in primates and fruit flies. *BMC Genomics* **17**: 617. doi:10.1186/s12864-016-2927-4
- Vieira C, Biémont C. 2004. Transposable element dynamics in two sibling species: *Drosophila melanogaster* and *Drosophila simulans*. *Genetica* **120**: 115–123. doi:10.1023/B:GENE.0000017635.34955.b5
- Vieira C, Lepetit D, Dumont S, Biémont C. 1999. Wake up of transposable elements following *Drosophila simulans* worldwide colonization. *Mol Biol Evol* **16**: 1251–1255. doi:10.1093/oxfordjournals.molbev.a026215
- Voelker RA. 1972. Preliminary characterization of “sex ratio” and rediscovery and reinterpretation of “male sex ratio” in *Drosophila affinis*. *Genetics* **71**: 597–606.
- Waring GL, Pollack JC. 1987. Cloning and characterization of a dispersed, multicopy, X chromosome sequence in *Drosophila melanogaster*. *Proc Natl Acad Sci* **84**: 2843–2847. doi:10.1073/pnas.84.9.2843
- Waterhouse RM, Seppey M, Simão FA, Manni M, Ioannidis P, Klioutchnikov G, Kriventseva EV, Zdobnov EM. 2017. BUSCO applications from quality assessments to gene prediction and phylogenomics. *Mol Biol Evol* **35**: 543–548. doi:10.1093/molbev/msx319
- Wei KHC, Lower SE, Caldas IV, Sless TJ, Barbash DA, Clark AG. 2018. Variable rates of simple satellite gains across the *Drosophila* phylogeny. *Mol Biol Evol* **35**: 925–941. doi:10.1093/molbev/msy005. msy005–msy005.
- Werren JH, Nur U, Wu CI. 1988. Selfish genetic elements. *Trends Ecol Evol* **3**: 297–302. doi:10.1016/0169-5347(88)90105-X
- Wu C-I. 2001. The genic view of the process of speciation. *J Evol Biol* **14**: 851–865. doi:10.1046/j.1420-9101.2001.00335.x
- Yang H-P, Barbash DA. 2008. Abundant and species-specific DINE-1 transposable elements in 12 *Drosophila* genomes. *Genome Biol* **9**: R39. doi:10.1186/gb-2008-9-2-r39
- Young MW, Schwartz HE. 1981. Nomadic gene families in *Drosophila*. *Cold Spring Harb Symp Quant Biol* **45** Pt 2: 629–640. doi:10.1101/SQB.1981.045.01.081
- Zhou Q, Zhang G, Zhang Y, Xu S, Zhao R, Zhan Z, Li X, Ding Y, Yang S, Wang W. 2008. On the origin of new genes in *Drosophila*. *Genome Res* **18**: 1446–1455. doi:10.1101/gr.076588.108
- Zimin AV, Marçais G, Puiu D, Roberts M, Salzberg SL, Yorke JA. 2013. The MaSuRCA genome assembler. *Bioinformatics* **29**: 2669–2677. doi:10.1093/bioinformatics/btt476

Received March 12, 2020; accepted in revised form December 28, 2020.